Molecular Therapy
Original Article

Combination of lentiviral and genome editing technologies for the treatment of sickle cell disease

Sophie Ramadier,[1,2,3] Anne Chalumeau,[1,2] Tristan Felix,[1,2] Nadia Othman,[3] Sherazade Aknoun,[3] Antonio Casini,[4] Giulia Maule,[4] Cecile Masson,[5] Anne De Cian,[6] Giacomo Frati,[1,2] Megane Brusson,[1,2] Jean-Paul Concordet,[6] Marina Cavazzana,[2,7,8] Anna Cereseto,[4] Wassim El Nemer,[9,10,11] Mario Amendola,[12] Benoit Wattellier,[3] Vasco Meneghini,[1,2,13] and Annarita Miccio[1,2]

[1]Laboratory of Chromatin and Gene Regulation during Development, Imagine Institute, INSERM UMR1163, 75015 Paris, France; [2]Université de Paris, 75015 Paris, France; [3]Phasics, Bâtiment Explorer, Espace Technologique, Route de l'Orme des Merisiers, 91190 St. Aubin, France; [4]CIBIO, University of Trento, 38100 Trento, Italy; [5]Paris-Descartes Bioinformatics Platform, Imagine Institute, 75015 Paris, France; [6]INSERM U1154, CNRS UMR7196, Museum National d'Histoire Naturelle, 75015 Paris, France; [7]Imagine Institute, 75015 Paris, France; [8]Biotherapy Department and Clinical Investigation Center, Assistance Publique Hôpitaux de Paris, INSERM, 75015 Paris, France; [9]Etablissement Français du Sang PACA-Corse, Marseille, France; [10]Aix Marseille Université, EFS, CNRS, ADES, "Biologie des Groupes Sanguins," 13000 Marseille, France; [11]Laboratoire d'Excellence GR-Ex, Paris, France; [12]Genethon, INSERM UMR951, 91000 Evry, France

Sickle cell disease (SCD) is caused by a mutation in the β-globin gene leading to polymerization of the sickle hemoglobin (HbS) and deformation of red blood cells. Autologous transplantation of hematopoietic stem/progenitor cells (HSPCs) genetically modified using lentiviral vectors (LVs) to express an anti-sickling β-globin leads to some clinical benefit in SCD patients, but it requires high-level transgene expression (i.e., high vector copy number [VCN]) to counteract HbS polymerization.

Here, we developed therapeutic approaches combining LV-based gene addition and CRISPR-Cas9 strategies aimed to either knock down the sickle β-globin and increase the incorporation of an anti-sickling globin (AS3) in hemoglobin tetramers, or to induce the expression of anti-sickling fetal γ-globins. HSPCs from SCD patients were transduced with LVs expressing AS3 and a guide RNA either targeting the endogenous β-globin gene or regions involved in fetal hemoglobin silencing. Transfection of transduced cells with Cas9 protein resulted in high editing efficiency, elevated levels of anti-sickling hemoglobins, and rescue of the SCD phenotype at a significantly lower VCN compared to the conventional LV-based approach.

This versatile platform can improve the efficacy of current gene addition approaches by combining different therapeutic strategies, thus reducing the vector amount required to achieve a therapeutic VCN and the associated genotoxicity risk.

INTRODUCTION

β-Hemoglobinopathies are severe anemias affecting ~350,000 newborns each year.[1] Sickle cell disease (SCD) is caused by a point mutation in the sixth codon of the β-globin gene (*HBB*), which leads to the E6V substitution. Hemoglobin tetramers containing the defective sickle β^S-globin (HbS) polymerize under hypoxia, and red blood cells (RBCs) assume a sickle shape and become inflexible. Sickle RBCs have a short half-life and obstruct microvessels, causing a chronic multi-organ disease associated with poor quality of life and short life expectancy.[2] β-Thalassemia is caused by mutations that reduce or abrogate β-globin production. The uncoupled α-globin chains cause apoptosis of erythroid precursors and hemolytic anemia.

Current treatments of SCD and β-thalassemia include regular RBC transfusions, which are associated with significant side effects, such as iron overload and organ damage. The only definitive cure for β-hemoglobinopathies is the allogeneic hematopoietic stem cell (HSC) transplantation from human leukocyte antigen (HLA)-matched sibling donors, which is available only to a fraction of the patients, requires an immunosuppressive regiment, and can be associated with chronic graft-versus-host disease.[3,4] Transplantation of autologous HSCs transduced with lentiviral vectors (LVs) carrying an anti-sickling β-globin transgene (i.e., encoding a β-globin chain inhibiting Hb polymerization) is a promising therapeutic option for patients lacking a compatible donor.[5,6] In particular, early data demonstrated a clinical benefit in a SCD patient transplanted with HSCs genetically corrected with a LV expressing a β-globin chain containing a single anti-sickling amino acid (Q at position 87, derived from the natural

Received 15 June 2021; accepted 9 August 2021;
https://doi.org/10.1016/j.ymthe.2021.08.019.

[13]Present address: San Raffaele Telethon Institute for Gene Therapy (SR-Tiget), IRCCS San Raffaele Scientific Institute, 20132 Milan, Italy

Correspondence: Annarita Miccio, Laboratory of Chromatin and Gene Regulation during Development, Imagine Institute, INSERM UMR 1163, 24 Boulevard du Montparnasse, 75015 Paris, France.
E-mail: annarita.miccio@institutimagine.org
Correspondence: Vasco Meneghini, San Raffaele Telethon Institute for Gene Therapy (SR-Tiget), IRCCS San Raffaele Scientific Institute, Via Olgettina 60, 20132 Milan, Italy.
E-mail: meneghini.vasco@hsr.it

anti-sickling fetal γ-globin).[7] However, the analysis of larger cohorts of patients showed that this treatment is only partially effective in the case of poor transgene transfer in HSCs,[8] which results in therapeutic β-globin levels insufficient to compete with β^S-globin for the incorporation into the Hb tetramers. Therefore, the achievement of clinically relevant transgene expression in SCD patients required a high number of integrated LV copies per cell, which could increase the potential genotoxicity risks associated to LV semi-random integration in the genome.[9,10] We have recently optimized a high-titer β-globin-expressing LV (currently used in a clinical trial for β-thalassemia[11]) for the treatment of SCD by introducing three anti-sickling amino acids substitutions (G16D, E22A, T87Q) in the β-globin chain (AS3),[12] which prevent the formation of axial and lateral contacts necessary for the generation of Hb polymers and increase the affinity for α-globin compared to the β^S-globin.[6,13] However, despite these improvements, the RBC sickling phenotype was only partially corrected even in the presence of a high vector copy number (VCN).[6]

Genome editing approaches have been recently developed for the treatment of β-hemoglobinopathies. Strategies based on the high-fidelity homology-directed repair (HDR) pathway have been exploited to correct the SCD mutation by providing a DNA donor template containing the wild-type (WT) β-globin sequence.[14–16] However, the efficiency of HDR-mediated gene correction is limited in HSCs, and gene disruption by non-homologous end joining (NHEJ), a more active DNA repair pathway in HSCs,[17] may be more frequent, generating a β-thalassemic phenotype instead of correcting the SCD mutation.[18]

The clinical severity of SCD and β-thalassemia is alleviated by the co-inheritance of mutations causing fetal γ-globin expression in adult RBCs (a condition termed hereditary persistence of fetal hemoglobin [HPFH][19]). The NHEJ pathway has been exploited to induce fetal γ-globin re-activation by disrupting *cis*-regulatory silencer regions in the γ-globin (*HBG*) promoters[20–23] (e.g., binding sites for BCL11A and LRF transcriptional repressors) and in the β-globin locus,[24] or to downregulate the BCL11A HbF repressor by targeting its erythroid-specific enhancer.[25–27] The extent and impact of HbF reactivation on the recovery of SCD and β-thalassemic phenotypes is currently under investigation in clinical studies.[28]

Overall, these pre-clinical and clinical studies show that gene therapy approaches for β-hemoglobinopathies require highly efficient genetic modification of HSCs and robust expression of therapeutic globins to achieve clinical benefit.

In this study, we developed a novel LV platform based on the concomitant expression of the anti-sickling AS3 transgene and a single guide RNA (sgRNA) targeting the *HBB* gene to induce the downregulation of the endogenous β^S globin in SCD erythroid cells and favor the incorporation of the therapeutic AS3 β-globin chain into Hb tetramers. The versatility of this platform was exploited by combining the AS3 expression with γ-globin re-activation induced by CRISPR-Cas9-mediated disruption of the BCL11A binding site in the *HBG* promoters or BCL11A downregulation, thus potentially extending its application to the treatment of β-thalassemia.

Our results demonstrate that editing the *HBB* gene or the *HBG* promoters is safe and enhances the therapeutic effect of the AS3 gene addition strategy, correcting the SCD pathological phenotype with a limited number of vector copies per cell.

RESULTS

Selection of an efficient sgRNA downregulating *HBB* expression

To select a sgRNA able to efficiently and safely knock down the mutant sickle *HBB* gene, we tested sgRNAs recognizing sequences within *HBB* exon 1 (gR-A, gR-B, gR-C, gR-D[29,30]) (Figure 1A). Plasmids expressing the different sgRNAs under the control of the human U6 promoter were individually delivered together with a plasmid carrying *SpCas9* nuclease fused with the green fluorescent protein (Cas9-GFP) in fetal K562 and adult HUDEP-2 erythroid cell lines.[31] The frequency of insertion and deletions (indels) ranged from ∼40% to ∼80% (Figure 1B), as measured by Sanger sequencing and tracking of indels by decomposition (TIDE) analysis.[32] The frequency of out-of-frame mutations (likely causing a decreased *HBB* expression) was substantially higher for gR-C and gR-D (70%–95%) than for gR-A and gR-B (25%–60%) in both K562 and HUDEP-2 cell lines (Figure 1C).

The ability of the different sgRNAs to downregulate *HBB* expression was evaluated in HUDEP-2 cells (expressing mainly adult β-globin) differentiated in mature erythroid precursors. qRT-PCR and western blot analysis showed a strong downregulation of β-globin expression at both mRNA (70%–85%) and protein (70%–90%) levels in comparison to HUDEP-2 cells transfected only with the Cas9-GFP plasmid (Figures 1D and 1E). Of note, all of the gRNAs generated premature stop codons (data not shown) that likely cause mRNA degradation through nonsense-mediated decay. As expected from editing data, gR-C and gR-D caused a more robust β-globin downregulation compared to gR-A and gR-B (Figures 1D and 1E). Of note, sgRNAs targeting the *HBB* gene did not alter mRNA expression of the other β-like globin genes (i.e., adult *HBD* and fetal *HBG* genes; Figure 1D), suggesting a specific targeting of the *HBB* coding sequence. Reversed-phase high-pressure liquid chromatography (RP-HPLC) and cation-exchange HPLC (CE-HPLC) analyses of differentiated HUDEP-2 cells treated with gR-C showed a decrease in β-globin production, resulting in an imbalance between α-globin and non-α-globin chains and accumulation of α-globin precipitates, a typical hallmark of β-thalassemia (Figures S1A and S1B). Notably, the presence of δ- and γ-globin chains was not sufficient to compensate for the lack of β-globin (Figure S1A).

The off-target activity of the best performing sgRNAs (gR-C and gR-D) was initially evaluated in the *HBD* gene, the *HBB* paralog with the highest sequence homology, which is often reported as the major off-target locus when targeting the *HBB* gene.[33] gR-C and gR-D target sequences have four and two mismatches with the potential off-target loci in *HBD* exon 1 (Figure S1C). TIDE analysis showed an absence

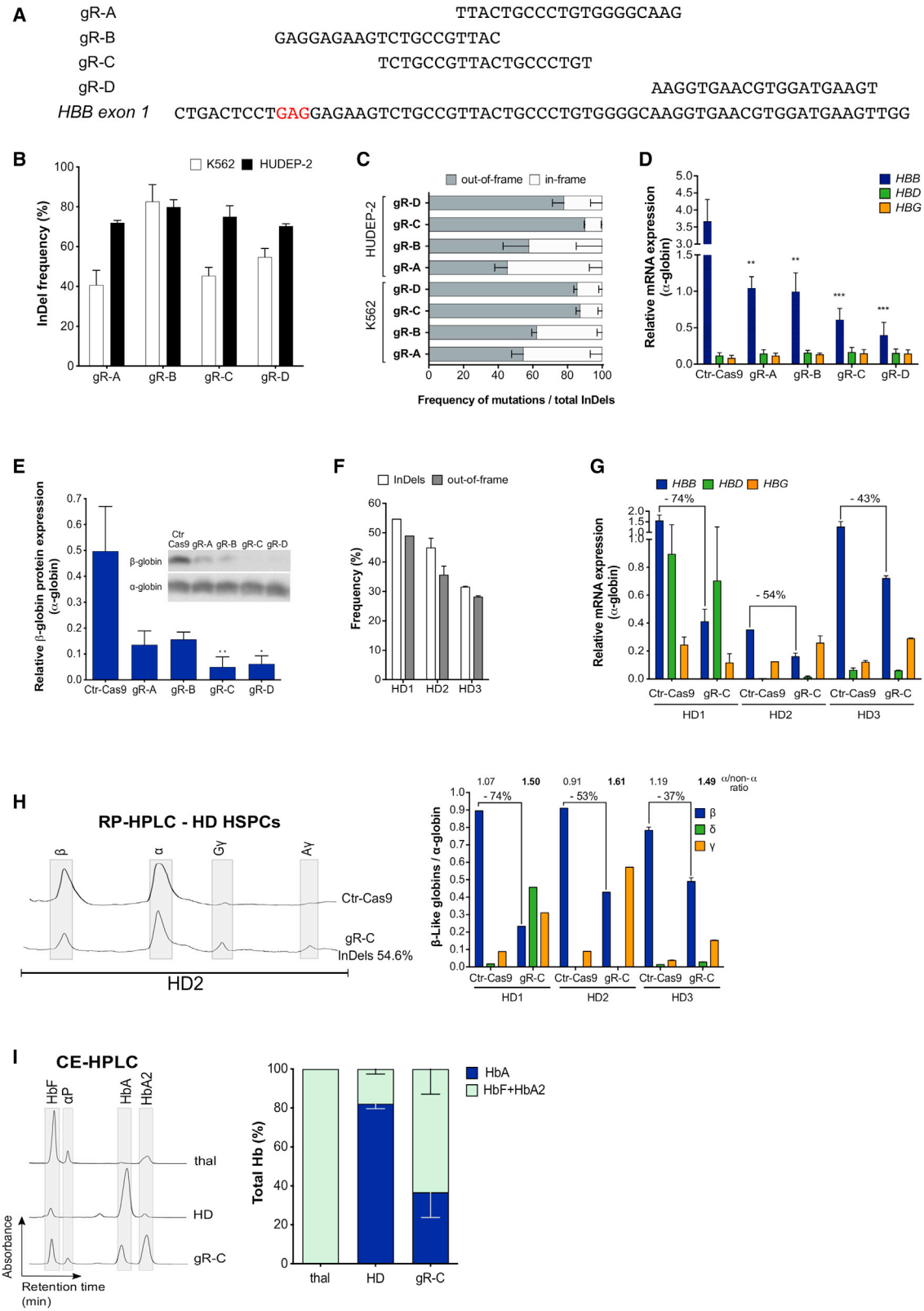

(legend on next page)

of indels in the *HBD* loci in both K562 and HUDEP-2 cells treated with gR-C or gR-D (Figure S1C). However, plasmid delivery of the CRISPR-Cas9 system in primary healthy donor (HD) hematopoietic stem/progenitor cells (HSPCs) resulted in ~3% of edited *HBD* alleles in gR-D-treated cells, while no off-target events in the *HBD* locus were detected in samples transfected with gR-C (Figure S1C). These findings are in line with the lower number of mismatches between the gR-D target sequence and the *HBD* off-target locus as compared to gR-C (Figure S1C). Based on these findings, we further characterized the off-target activity of gR-C in plasmid-transfected HUDEP-2 cells and primary HD HSPCs by analyzing the top-15 off-targets predicted by COSMID[34] (Table S2). TIDE analysis revealed no off-target activity in 14 out of 15 loci, including *HBD* and *HBG* genes. Indels were detected only at the off-target locus 4 (OT4) in HUDEP-2 cells (~2% indels) and at relatively low levels in primary HSPCs (~0.6% indels) (Figure S1D). However, this off-target maps to an intergenic region, which does not contain known hematopoietic *cis*-regulatory regions (Figure S1E).

The gR-C was selected for further analyses aimed at evaluating β-globin downregulation in HSPC-derived erythroid cells, because of its high on-target activity and low off-target editing. We transfected adult HD HPSCs with plasmids encoding gR-C and Cas9-GFP, and fluorescence-activated cell sorting (FACS)-sorted Cas9-GFP$^+$ cells were differentiated toward the erythroid lineage. Genome editing efficiency ranged from 32% to 54% of indels with 30%–49% of out-of-frame mutations in HSPC-derived erythroid cells (Figures 1F; Figure S1F). We observed β-globin downregulation at both mRNA and protein levels, which was well correlated with the frequency of frameshift mutations (Figures 1F–1H). In HSPC-derived erythroid cells, RP-HPLC analysis revealed that β-globin downregulation induced an imbalance between the α- and β-like globin chains, which was not compensated by the presence of γ (Aγ+Gγ)-globin and δ-globin chains (Figure 1H). Importantly, CE-HPLC analysis demonstrated that gR-C led to a substantial reduction of HbA tetramers and accumulation of α-globin precipitates (Figure 1I).

Overall, these data showed that gR-C is efficient in generating frameshift mutations in *HBB*, leading to a robust downregulation of β-globin synthesis in both erythroid cell lines and primary cells.

A bifunctional LV to concomitantly express the AS3 anti-sickling globin and downregulate the endogenous β-globin

Transduction of HSPCs isolated from SCD patients with a LV carrying the anti-sickling AS3-globin transgene (LV AS3) led to a partial correction of the SCD phenotype of HSPC-derived RBCs.[6] To enhance the therapeutic efficacy of gene addition strategies, we introduced a gR-C expression cassette in LV AS3 to concomitantly induce the expression of the AS3 transgene and the knockdown of the endogenous β-globin gene upon transient Cas9 delivery, thus favoring the incorporation of the AS3-globin chain into Hb tetramers. Importantly, the combination of gene addition and gene silencing strategies allows the knockdown of the mutant sickle β-globin gene only in cells expressing the therapeutic β-globin chain, which will compensate for the HbS reduction, thus avoiding the potential generation of a β-thalassemic phenotype.

The sgRNA expression cassette was inserted downstream of the AS3-expressing cassette in reverse orientation to the AS3 transgene transcription (Figure 2A). To further increase gR-C editing efficiency,

Figure 1. Test and validation of an effective sgRNA to knock down the *HBB* gene

(A) sgRNAs are aligned to their complementary on-target loci on exon 1 of the *HBB* gene. gR-B targets a region containing the SCD mutation, and therefore its sequence was modified to target the WT *HBB* gene during the validation experiments in K562 and HUDEP-2 erythroid cell lines, and in HD HSPCs. The codon containing the SCD mutation is highlighted in red. (B) Editing efficiency by TIDE analysis after PCR amplification of the target region and Sanger sequencing in Cas9-GFP$^+$ K562 (n = 3 for gR-A, 4 for gR-B, 6 for gR-C, and 5 for gR-D) and HUDEP-2 (n = 5 for gR-C; n = 4 for gR-A, gR-B, and gR-D) erythroid cell lines. Transfection efficiency was 55%–70% for K562 and 30%–60% for HUDEP-2. Data are expressed as mean ± SEM. (C) Out-of-frame mutations identified using TIDE after PCR amplification of the target region and Sanger sequencing in K562 (n = 3 for gR-A, 4 for gR-B, 6 for gR-C, and 5 for gR-D) and HUDEP-2 (n = 5 for gR-C; n = 4 for gR-A, gR-B, and gR-D) erythroid cell lines. Data are expressed as mean ± SEM. The frequency of out-of-frame mutations for gR-C was significantly higher than for gR-A ($p < 0.0001$ in K562 and $p < 0.05$ in HUDEP-2) and gR-B ($p < 0.005$ in K562). In K562, the frequency of out-of-frame mutations for gR-D was significantly higher than for gR-A and gR-B ($p < 0.0005$). In both K562 and HUDEP-2, no differences were observed between gR-C and gR-D (one-way ANOVA test: Tukey's multiple comparisons test). (D) Relative expression of *HBB*, *HBD*, and *HBG* mRNAs normalized to α-globin, detected by qRT-PCR in HUDEP-2 cells. Data are expressed as mean ± SEM (n = 3). **$p < 0.01$ between gR-A or gR-B versus control (Ctr)-Cas9; ***$p < 0.001$ between gR-C or gR-D versus Ctr-Cas9 (two-way ANOVA test: Dunnett's multiple comparisons test). Ctr-Cas9 samples are HUDEP-2 cells transfected only with the Cas9-GFP plasmid. (E) Relative expression of the β-globin chain normalized to the α-globin chain, as measured by western blot analysis in differentiated HUDEP-2 cells. Data are expressed as mean ± SEM (n = 4 for gR-C; n = 3 for gR-A, gR-B, and gR-D). *$p < 0.05$ and **$p < 0.01$ versus Ctr-Cas9 (two-way ANOVA test: Sidak's multiple comparisons test). A representative western blot image is shown. Ctr-Cas9 samples are HUDEP-2 cells transfected only with the Cas9-GFP plasmid. (F) Editing efficiency (indels) and frequency of out-of-frame mutations measured by TIDE analysis after PCR amplification of the target region and Sanger sequencing in G-CSF-mobilized peripheral blood (mPB) HD HSPCs edited with gR-C (n = 1 for HD1, n = 2 for HD2, and n = 2 for HD3). Data are expressed as mean ± SEM. (G) Relative expression of *HBB*, *HBD*, and *HBG* mRNAs normalized to α-globin, measured by qRT-PCR in erythroid cells derived from G-CSF-mPB HD HSPCs transfected with Cas9-GFP plasmid only (Ctr-Cas9) or with both Cas9-GFP and gR-C plasmids (gR-C). *HBB* decrease upon gR-C treatment is reported as percentage above the histogram bars (n = 1 for HD1, n = 2 for HD2, and n = 2 for HD3). Data are expressed as mean ± SEM. (H) RP-HPLC quantification of globin chains in erythroid cells derived from G-CSF-mPB HD HSPCs transfected with Cas9-GFP plasmid only (Ctr-Cas9) or with both Cas9-GFP and gR-C plasmids (gR-C). β-Like globin chains are normalized over α-globin chains (n = 1 for HD1, n = 2 for HD2, and n = 2 for HD3; n = 5 biological replicates). The percentage of β-globin decreases upon gR-C treatment and the α-globin/non-α-globin ratio is reported above the histogram bars. Data are expressed as mean ± SEM. A representative chromatogram is reported in the left panel. (I) CE-HPLC analysis of Hb tetramers in β-thalassemic cells (thal) and in erythroid cells derived from G-CSF-mPB HD HSPCs treated or not with gR-C. gR-C-treated samples have a hemoglobin expression pattern similar to the profile observed in *in vitro*-differentiated erythroid cells from a β-thalassemia patient. We calculated the percentage of Hb types over the total Hb tetramers (n = 2 donors). CE-HPLC chromatograms are reported on the left panel. αp, α-precipitates. Data are expressed as mean ± SEM.

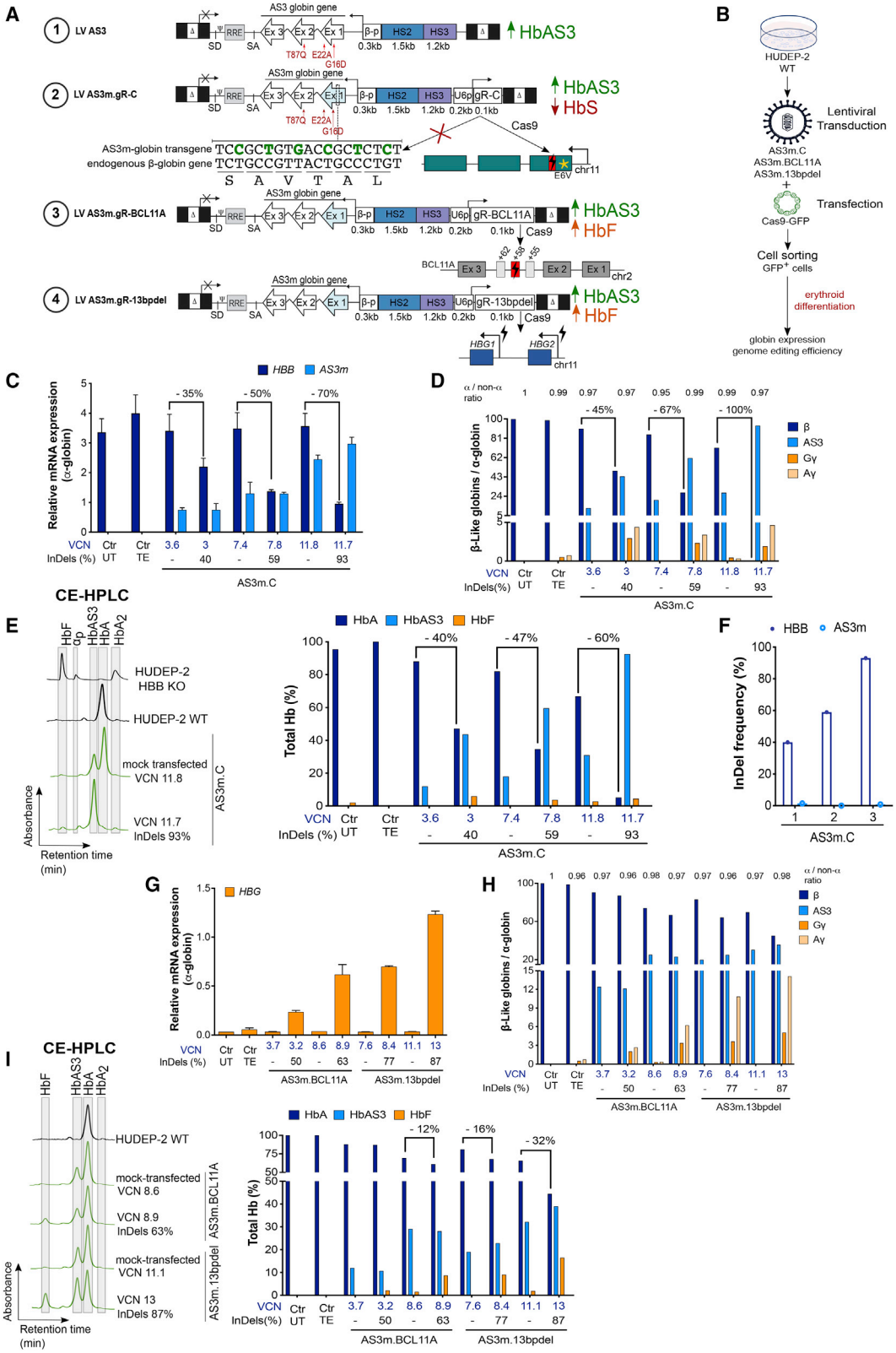

(legend on next page)

we used an optimized sgRNA scaffold carrying a mutation in the RNA polymerase (Pol) II transcription pause sequence and an extended sgRNA duplex to increase U6-driven sgRNA transcription and sgRNA-Cas9 interactions, respectively.[35] Plasmid transfection of both K562 cells and adult HD HSPCs showed that the use of the optimized scaffold increased indel frequency, while maintaining a similar percentage of out-of-frame mutations (~90%) compared to the original scaffold (Figures S1G and S1H). To avoid the downregulation of transgene expression, we introduced six silent mutations in the AS3 sequence complementary to gR-C (AS3m transgene) using synonymous codons commonly found in β-like globin genes (Figure 2A). These silent mutations are expected to impair AS3m targeting and editing by gR-C, which will then recognize only the endogenous β-globin gene. The insertion of the sgRNA expression cassette did not compromise LV titer (~10^9 transduction unit [TU]/mL) and infectivity (~7×10^4 TU/ng p24) (LV AS3m.C vector; Figure S2A).

To evaluate whether the silent mutations impair the production of AS3 chains, we compared LVs harboring the original (LV AS3) or the modified (LV AS3m) AS3 transgene in a β-thalassemic HUDEP-2 cell line[36] (HBB knockout [KO]). In differentiated HBB KO HUDEP-2 cells, β-globin expression is abolished, resulting in the imbalance between α and non-α chains and accumulation of α-globin precipitates (Figures S2B and S2C). We transduced HBB KO HUDEP-2 cells with LV AS3 and LV AS3m at increasing multiplicities of infection (MOIs) obtaining a VCN ranging from 0.5 to ~9 (Figures S2B and S2C). HPLC analyses showed that AS3 expression was comparable in LV AS3- and LV AS3m-transduced erythroid precursors harboring a similar VCN (Figures S2B and S2C). Both LVs partially restored the β-thalassemic phenotype in cells harboring a low VCN (0.5–0.9), while a higher gene marking (VCN > 4) fully corrected the α-globin/non-α-globin imbalance, as evaluated by RP-HPLC (Figure S2B). These results demonstrated that the silent mutations in the modified transgene do not affect AS3 expression and the production of functional HbAS3 tetramers.

To test the capability of LV AS3m.C to downregulate the expression of the endogenous *HBB* gene, WT HUDEP-2 cells were transduced with increasing doses of LV AS3m.C and then either transfected with the Cas9-GFP-expressing plasmid or mock transfected. FACS-sorted Cas9-GFP$^+$ cells were then differentiated into mature erythroblasts (Figure 2B). The indel frequency at the on-target *HBB* gene was positively correlated with the VCN (Figure 2C). *HBB* editing resulted in the knockdown of the endogenous β-globin at both mRNA and protein levels, with higher indel frequency resulting in more robust downregulation of *HBB* expression (Figures 2C–2E). Of note, no indels were detected in the AS3m transgene even in samples displaying a high on-target activity at the endogenous *HBB* gene, demonstrating that silent mutations in AS3m avoid its targeting by gR-C, which specifically recognizes the endogenous β-globin gene (Figure 2F). Concordantly, AS3m mRNA levels were comparable between the control and edited samples (Figure 2C). Importantly, the downregulation of the endogenous β-globin expression favored incorporation of the AS3 globin chain into the Hb tetramers (Figure 2E). In cells harboring a relatively low gene marking (VCN of 3 associated with an editing efficiency of 40%), this resulted in a balance between HbA and HbAS3 tetramers, which could not be reached in unedited cells even at high VCN (11.8; Figure 2E). Notably, the reduction of the

Figure 2. Combination of lentiviral and genome editing technologies is efficient in HUDEP-2 cells

(A) Schematic representation of the LVs carrying either the AS3 globin gene (LV AS3, strategy #1) or the AS3m globin gene and a sgRNA-expressing cassette (LV AS3m.gR). Both AS3- and AS3m-globin genes are under the control of a short β-globin promoter (β-p) and a mini-βLCR containing HS2 and HS3. The anti-sickling amino acid substitutions are reported in red. The modified nucleotides in LV AS3m, avoiding its targeting by the gR-C, are reported in green. We indicated the amino acids below the nucleotide sequence. sgRNA expression is under the control of the human U6 promoter (U6p). gR-C targets a region in exon 1 (Ex1) of HBB (strategy #2), gR-BCL11A targets the +58-kb erythroid-specific enhancer of *BCL11A* (strategy #3), and gR-13bpdel targets the BCL11A binding site within the *HBG* promoters (strategy #4). (B) Schematic representation of the LV transduction and plasmid transfection protocol used in HUDEP-2 cells. Cells were transduced with LV AS3m carrying gR-C, BCL11A, and 13bpdel sgRNAs and transfected after 10 days with a Cas9-GFP plasmid. Transfection efficiency was 30%–60%. FACS-sorted Cas9-GFP$^+$ cells were differentiated into mature erythroblasts. (C) Relative expression of *HBB* and *AS3m* mRNAs normalized to α-globin, as detected by qRT-PCR. VCN values are reported in blue and indels in black below the graph. Ctr UTs are untreated HUDEP-2 cells and Ctr TEs are HUDEP-2 cells transfected only with TE buffer. Transduced samples that were mock transfected are indicated with "–." The percentage of *HBB* decrease upon LV AS3m.C treatment is reported above the histogram bars. Data are expressed as mean ± SEM. (D) RP-HPLC quantification of globin chains in Cas9-treated and control (mock-transfected) LV AS3m.C-transduced cells. β-Like globin chains were normalized to α-globin chains. VCN values are reported in blue and indels in black below the graph. Ctr UTs are untreated HUDEP-2 cells and Ctr TEs are HUDEP-2 cells transfected only with TE buffer. Transduced samples that were mock transfected are indicated with "–" and harbored no indels. The percentage of β-globin decrease upon LV AS3m.C treatment and the α-globin/non-α-globin ratio are reported above the histogram bars. (E) CE-HPLC chromatograms (left panel) and quantification (right panel) of Hb tetramers in Cas9-treated and control mock-transfected LV AS3m.C-transduced cells. We calculated the percentage of each Hb type over the total Hb tetramers. VCN values are reported in blue and indels in black below the graph. Ctr UTs are untreated HUDEP-2 cells and Ctr TEs are HUDEP-2 cells transfected only with TE buffer. The decrease in HbA expression upon LV AS3m.C treatment is reported as percentage above the histogram bars. (F) Editing efficiency (indel frequency) in LV AS3m.C-treated HUDEP-2 cells measured by TIDE analysis after PCR amplification and Sanger sequencing of the target region in *HBB* exon 1 and the potential off-target region in the transgene (AS3m) in Cas9-GFP$^+$ HUDEP-2 erythroid cells. (G) Relative *HBG* expression normalized to α-globin, as detected by qRT-PCR in Cas9-treated and mock-transfected cells transduced with LV AS3m.BCL11A or LV AS3m.13bpdel. VCN values are reported in blue and indels in black below the graph. Ctr UTs are untreated HUDEP-2 cells and Ctr TEs are HUDEP-2 cells transfected only with TE buffer. Data are expressed as mean ± SEM. (H) RP-HPLC quantification of globin chains in Cas9-treated and mock-transfected cells transduced with LV AS3m.BCL11A or LV AS3m.13bpdel. β-Like globin chains are normalized over α-globin. VCN values are reported in blue and indels in black below the graph. α-Globin/non-α-globin ratios are reported above the histogram bars. Ctr UTs are untreated HUDEP-2 cells and Ctr TEs are HUDEP-2 cells transfected only with TE buffer. (I) CE-HPLC chromatograms (left panel) and quantification (right panel) of Hb tetramers in Cas9-treated and mock-transfected LV AS3m.BCL11A- and LV AS3m.13bpdel-transduced cells. We plotted the percentage of each Hb type over the total Hb tetramers. VCN values are reported in blue and indels in black below the graph. The percentage of HbA decrease is reported above the histogram bars. Ctr UTs are untreated HUDEP-2 cells and Ctr TEs are HUDEP-2 cells transfected only with TE buffer.

β-globin chain content was compensated by the AS3-globin production and incorporation into the Hb tetramers, thus avoiding the imbalance between the α and non-α chains and the formation of α-precipitates (Figures 2D and 2E). Accordingly, the erythroid differentiation of HUDEP-2 cells was not impacted by editing of the *HBB* gene, as the cell composition was similar in edited and control HUDEP-2 cells, while HBB KO HUDEP-2 cells showed a delay in differentiation typical of β-thalassemia[37] (Figure S3).

We achieved similar results using a clinically relevant, plasmid-free transfection protocol in LV-transduced WT HUDEP-2 cells. In particular, we compared Cas9-GFP plasmid or protein delivery methods in LV AS3m.C-transduced WT HUDEP-2 cells. Transfection with Cas9-GFP protein was less cytotoxic (68% ± 4% of alive cells in untransfected samples, 58% ± 4% and 37% ± 6% in samples transfected with 15 μg of Cas9-GFP protein and Cas9-GFP-expressing plasmid, respectively), more efficient (∼70% and 32.5% of GFP^+ cells upon protein and plasmid transfection, respectively), and led to a higher editing efficiency at the on-target *HBB* locus in unsorted bulk populations (Figure S4A). LV AS3m.C-transduced WT HUDEP-2 cells transfected with 15 μg of Cas9-GFP protein were terminally differentiated in mature erythroid precursors. The decrease of HbA levels and the concomitant increase of HbAS3 content were significantly correlated with the VCN (Figure S4B) and the genome editing efficiency at the *HBB* locus (Figure S4C). Importantly, similar amounts of HbA and HbAS3 were detected in cells harboring a VCN of ∼2.5% and ∼46% of edited alleles (Figures S4B and S4C). On the contrary, in mock-transfected LV AS3m.C-transduced cells, HbA content exceeded the levels of HbAS3 even in cells harboring a high VCN (Figure S4B).

Overall, these data showed that the treatment with LV AS3m.C can safely and efficiently downregulate the expression of the endogenous β-globin and increase the production of Hb tetramers containing the therapeutic AS3-globin compared to the classical gene addition approach.

A bifunctional LV to induce the expression of the anti-sickling AS3-globin and γ-globin chains

Considering the therapeutic benefit of high fetal γ-globin expression in SCD and β-thalassemia patients,[38–40] we exploited the flexibility of this novel LV platform to simultaneously express the AS3m transgene and reactivate HbF expression. The combined expression of AS3 and γ chains can elevate the total Hb content in β-thalassemia patients and, as both of these globins display anti-sickling properties, it can also benefit SCD patients.

We generated LVs expressing the AS3m transgene and a sgRNA that either disrupts a sequence in the *BCL11A* erythroid-specific enhancer critical for its expression (AS3m.BCL11A)[26] or generates 13-bp deletions encompassing the BCL11A binding site in the fetal γ-globin promoters (AS3m.13bpdel)[20] (Figure 2A). As observed for LV AS3m.C, the insertion of the sgRNA cassette did not impair LV titer and infectivity (Figure S2A).

WT HUDEP-2 cells were transduced with LV AS3m.BCL11A or LV AS3m.13bpdel and then transfected with Cas9-GFP plasmid or mock transfected. FACS-sorted Cas9-GFP^+ cells and control samples were differentiated in mature erythroid precursors (Figure 2B). Editing of the *BCL11A* enhancer or the γ-globin promoters did not impact the differentiation of HUDEP-2 cells (Figure S3). LV AS3m.BCL11A-transduced cells showed up to 63% of indel frequency at the *BCL11A* enhancer, which caused a strong decrease in the levels of *BCL11A-XL*, the isoform mainly involved in the inhibition of HbF expression[41,42] (Figure S5A). In LV AS3m.13bpdel-transduced cells, around one third (31.7% ± 0.5%) of the total editing events generated by gR-13bpdel were MMEJ-mediated 13-bp deletions removing the entire BCL11A binding site (Figure S5B). All other events also led to the disruption of the BCL11A binding site in the *HBG* promoters (Figure S5B). Editing of the BCL11A enhancer or the γ-globin promoters resulted in *HBG* gene induction, as well as increased γ-globin chain and HbF production (Figures 2G–2I). In particular, the concomitant expression of AS3 and γ-globin resulted in up to 37% and 55% of total anti-sickling hemoglobins (HbF+HbAS3) in LV AS3m.BCL11A- and LV AS3m.13bpdel-transduced cells, respectively (Figure 2I). The combined expression of HbF and HbAS3 decreased adult HbA production in samples with the higher genome editing frequencies (Figure 2I). Flow cytometry analysis confirmed the increased HbF production with up to 61% and 74% of F-cells in samples treated with LV AS3m.BCL11A and LV AS3m.13bpdel, respectively (Figure S5C).

These data show that CRISPR-Cas9-mediated induction of HbF expression can increase the total Hb content in cells expressing a β-globin therapeutic transgene, thus representing a promising strategy to correct both SCD and β-thalassemia phenotypes.

The combination of gene addition and genome editing approaches increased the content of anti-sickling hemoglobins in SCD RBCs

The efficacy and safety of our approach was evaluated in adult plerixafor-mobilized peripheral blood (mPB) HSPCs from SCD patients. HSPCs were transduced with increasing doses of LV AS3m.C and transfected 48 h later with Cas9-GFP protein using previously optimized protocols[6,43] (Figure 3A). Control and edited SCD HSPCs were plated in clonogenic cultures (colony forming cell [CFC] assay) allowing the growth of erythroid (burst-forming unit-erythroid cells [BFU-Es]) and granulomonocytic (colony-forming unit granulocyte-macrophages [CFU-GMs]) progenitors. The electroporation of transduced cells modestly reduced the number of progenitors, although this decrease was not statistically significant (Figure S6A). Importantly, no significant difference was observed between LV AS3m.C-transduced, mock-transfected, and edited samples (Figure S6A). Upon differentiation in mature erythroblasts, we observed a significant correlation between editing efficiency at the *HBB* locus and VCN, with an indel frequency ranging from 21% to 67% (Figure 3B). A positive correlation between editing frequency and VCN was also observed in pools of BFU-Es derived from SCD HSPCs treated with LV AS3m.C and Cas9-GFP protein (Figure S6B). As

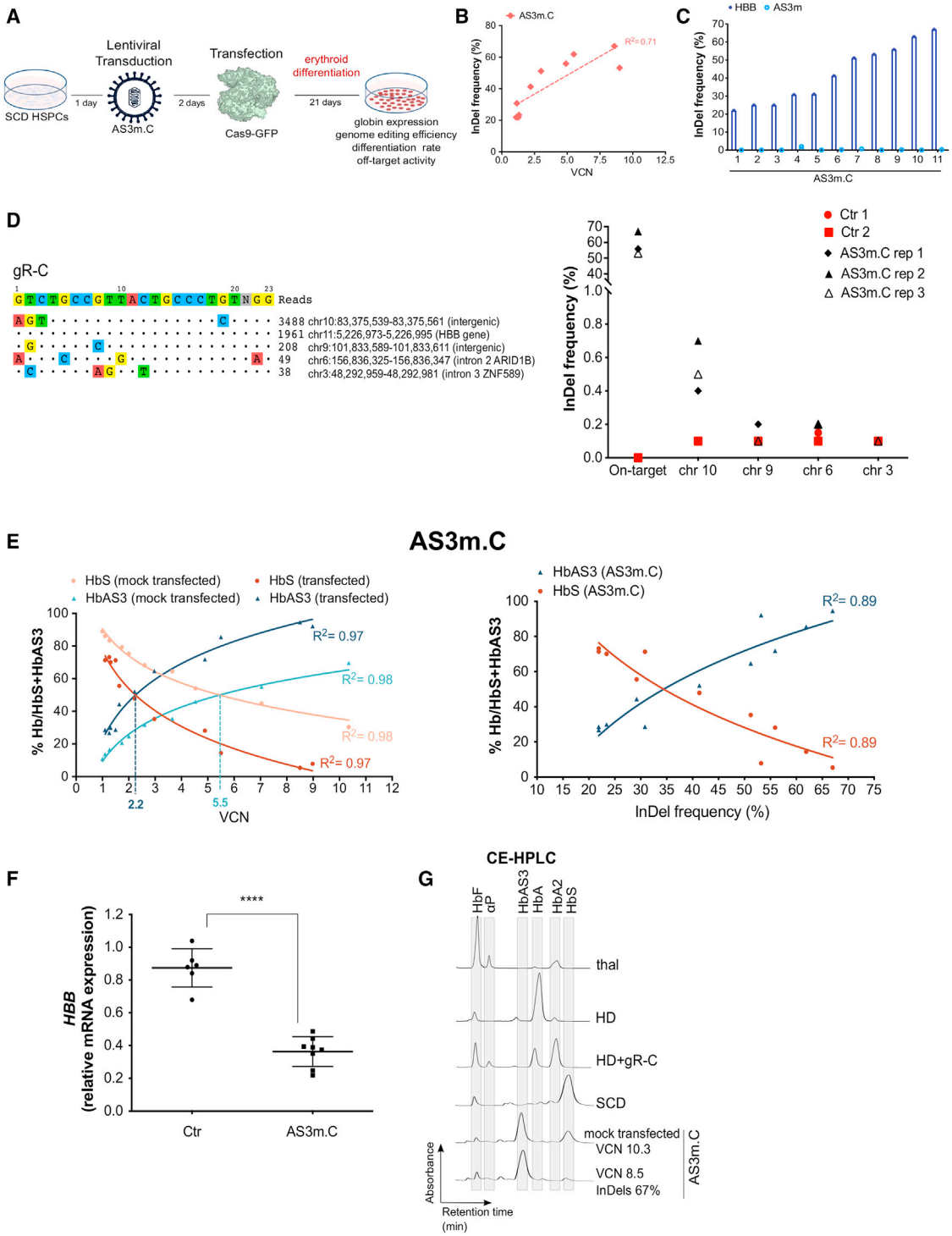

Figure 3. Testing of the bifunctional LV AS3m.C in SCD HSPCs

(A) Schematic representation of the protocol used to transduce and transfect SCD HSPCs. 24 h after thawing, HSPCs were transduced with LV AS3m.C and after 48 h cells were transfected with the Cas9-GFP protein and differentiated into mature RBCs following a 21-day differentiation protocol. (B) Correlation between VCN and indel frequency in cells treated with LV AS3m.C (two mobilized SCD donors). R^2 and line-of-best-fit equation are indicated. (C) Indel frequency in LV AS3m.C-treated SCD HSPCs measured by TIDE analysis after PCR amplification and Sanger sequencing of the target region in *HBB* exon 1 and the potential off-target region in the transgene (AS3m). (D) Evaluation of off-target activity. GUIDE-seq analysis of gR-C in 293T cells (left panel). The protospacer targeted by gR-C and the protospacer adjacent motifs (PAMs) are shown in the

(legend continued on next page)

previously observed in HUDEP-2 cells, no indels were detected in the sequence of the AS3m transgene in any of the treated samples (Figure 3C). Deep sequencing analysis in edited erythroblasts revealed a low off-target activity only in one out of the four off-target sites detected by GUIDE-seq (genome-wide unbiased identification of double-stranded breaks enabled by sequencing) analysis (Figure 3D). This locus corresponds to the OT4 previously identified in primary HSPCs by Sanger sequencing (Figures S1D and S1E).

Erythroblasts were further differentiated in enucleated RBCs using a three-phase protocol[44] (Figure 3A). We observed a positive correlation between VCN and the HbAS3 content in RBCs derived from mock-transfected, LV AS3m.C-transduced HSPCs achieving equivalent HbS and HbAS3 levels at a VCN of ~5.5 (Figure 3E). Cas9 treatment led to a decreased expression of the sickle *HBB* gene at both mRNA and protein levels, thus favoring the incorporation of the AS3 chain in Hb tetramers (Figures 3E and 3F; Figure S6C). Importantly, in RBCs derived from edited SCD HSPCs, similar amounts of HbS and HbAS3 were observed already at a VCN of ~2.2 (indel frequency of ~41%), reproducing the Hb profile of asymptomatic SCD carriers (Figure 3E). HbS downregulation and increased incorporation of the AS3 chain in Hb tetramers were still evident at low VCN (Figures 3E and 3F; Figure S6C). Notably, CE-HPLC showed an absence of α-globin precipitates in RBCs obtained from edited HSPCs, indicating that the expression of the AS3 chain was able to efficiently compensate for the lack of β^S-globin expression and avoid the generation of a β-thalassemic phenotype (Figure 3G).

In parallel, SCD mPB HSPCs were transduced with increasing doses of LV AS3m.13bpdel transfected with Cas9-GFP protein and then differentiated toward the erythroid lineage (Figure 4A). No significant differences were observed in the number of BFU-Es and CFU-GMs between control and edited samples (Figure S6A). We observed a direct correlation between VCN and indel frequency in BFU-Es and mature erythroblasts (Figure 4B; Figure S6B). LV AS3m.13bpdel-transduced erythroblasts showed ~30% of edited loci at a VCN of 3–4, and up to 50% at higher VCNs (Figure 4B; Figure S6B). On the contrary, SCD mPB HSPCs transduced with LV AS3m.BCL11A were poorly edited, reaching a maximum of ~20% of indel efficiency (Figure 4B). Deep-sequencing analyses of the only gR-13bpdel off-target previously detected by GUIDE-seq[23] revealed no off-target activity in LV AS3m.13bpdel-transduced erythroblasts (Figure 4C). GUIDE-seq analysis in 293T cells showed a high number of off-target sites for the sgRNA targeting the *BCL11A* enhancer (Figure 4D).

Given the low efficiency of LV AS3m.BCL11A and the high number of off-target sites, we further differentiated into enucleated RBCs only the cells derived from edited, LV AS3m.13bpdel-transduced HSPCs to evaluate the content of anti-sickling globins. The treatment of LV AS3m.13bpdel-transduced SCD HSPCs with Cas9-GFP protein led to an increased *HBG* mRNA expression (Figure 4E), reaching a percentage of F cells ranging from 40% to 85% (Figure 4F). CE-HPLC analysis showed that the total amount of anti-sickling hemoglobins (HbF+HbAS3) was positively correlated with the VCN and the editing frequency (Figures 4G and 4H). The concomitant AS3-globin chain expression and γ-globin reactivation resulted in reduced HbS levels (Figures 4G and 4H). Importantly, similar amounts of HbS and anti-sickling hemoglobins were obtained at a lower VCN (VCN of ~3.7; 34% of indels) in edited cells compared to the mock-transfected samples (VCN of ~5.4) (Figures 4G and 4H). Importantly, γ-globin reactivation was still observed in edited samples at low VCN (Figures 4G and 4H; Figure S6D).

The increased content of anti-sickling hemoglobins rescues the SCD cell phenotype

To assess the effect of the increased production of anti-sickling Hb tetramers on RBC sickling, we performed a deoxygenation assay to measure the proportion of sickle-shaped RBCs. *In vitro*-generated RBCs were exposed to an oxygen-deprived atmosphere, which induces HbS polymerization and RBC sickling. The percentage of sickled cells was decreased in RBC populations derived from mock-transfected, LV AS3m.C- and AS3m.13bpdel-transduced HSPCs compared to untreated SCD controls as a consequence of the expression of the AS3-globin chain, with 40%–60% of normal, doughnut-shaped RBCs at a VCN of ~2–3 (Figure 5). Interestingly, in RBCs derived from edited LV AS3m.C-transduced HSPCs, HbS downregulation combined with the high HbAS3 expression resulted in a substantial increase in the proportion of corrected RBCs (Figure 5). This effect was still evident by comparing RBCs generated from edited and mock-transfected LV AS3m.C-transduced HSPCs with a higher VCN (Figure 5). Finally, the increased HbF amount induced by the editing of the *HBG* promoters led to a modest but still significant reduction in the percentage of sickle-shaped RBCs compared to samples obtained from unedited, LV AS3m.13bpdel-transduced HSPCs showing a similar VCN (Figure 5).

Erythroid cell differentiation and RBC properties remain largely unchanged upon editing of SCD HSPCs

To exclude any impairment in erythroid differentiation of edited HSPCs, we monitored over time the erythroid liquid cultures using

first line. Off-targets and their mismatches with the on-target (highlighted in color), sequencing read counts, and chromosomal position are reported. Deep-sequencing analysis of off-target editing events in mature erythroblasts derived from SCD HSPCs treated with LV AS3m.C (right panel). Transduced and mock-transfected SCD cells (Ctr) are indicated in red and edited samples (AS3m.C) in black. (E) Correlation between VCN (left panel) or indel frequency (right panel) and percentage of HbS and HbAS3 (determined by CE-HPLC) in SCD RBCs derived from mock-transfected (orange and light blue) and Cas9-transfected (red and dark blue) SCD HSPCs transduced with LV AS3m.C (two mobilized SCD donors). R^2 and line-of-best-fit equation are indicated. Dashed lines indicate the VCN required to achieve equal amounts of HbS and HbAS3. (F) Relative expression of *HBB* mRNA normalized to α-globin in untreated SCD cells (Ctr) (n = 6) and in cells treated with LV AS3m.C (n = 8, 2 mobilized SCD donors). ****$p < 0.0001$ (unpaired t test). Horizontal lines indicate median and first and third quartiles. (G) Representative CE-HPLC chromatograms showing the Hb profile of *in vitro*-differentiated mature erythroblasts. From top to bottom: β-thalassemic cells (thal), healthy donor cells (HD), HD cells treated with gR-C plasmid (HD+gR-C), SCD cells (SCD), SCD cells transduced with LV AS3m.C and mock transfected, and SCD cells transduced with LV AS3m.C and transfected with Cas9-GFP protein.

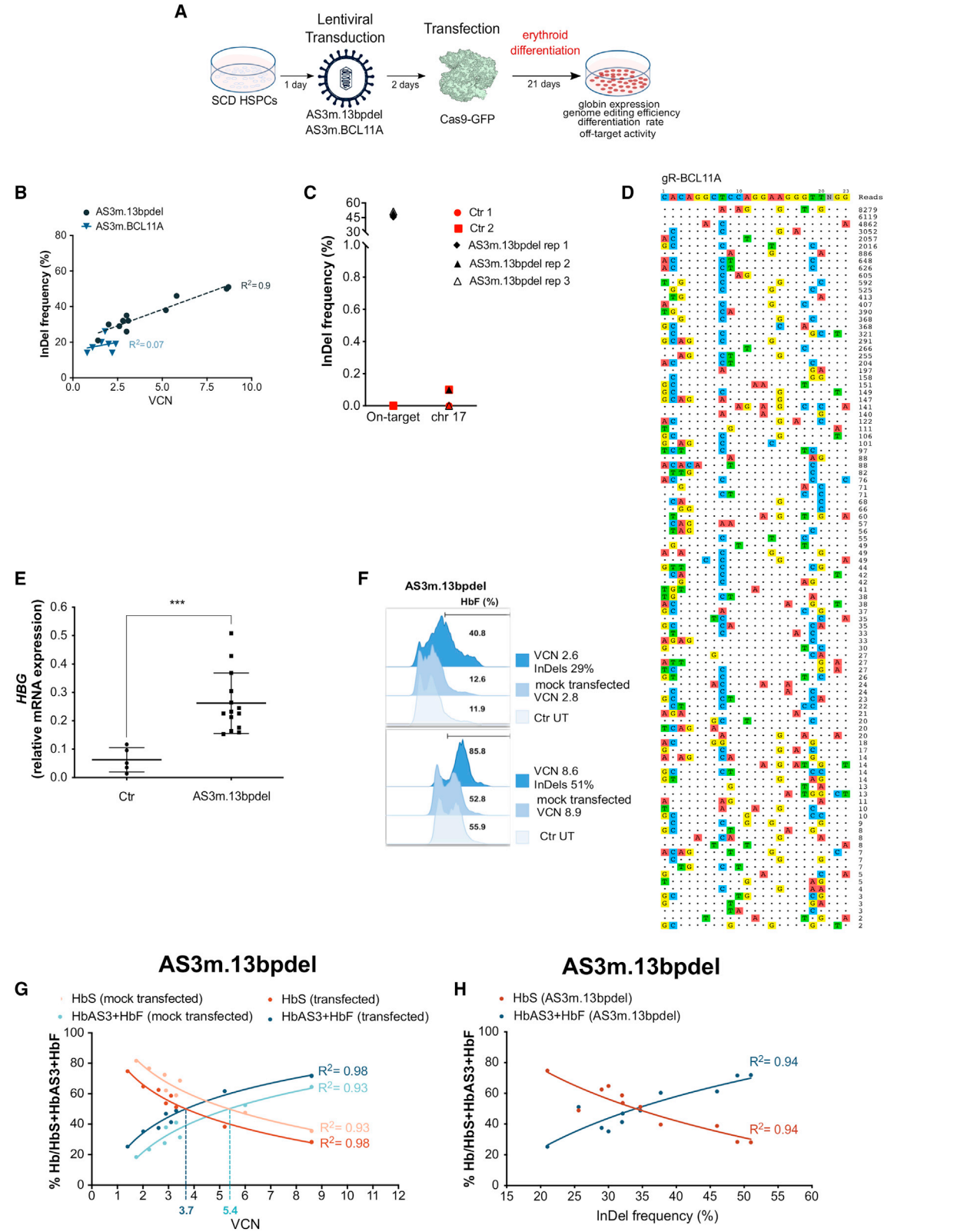

(legend on next page)

flow cytometry and quantitative phase imaging. In particular, although the co-expression of the AS3-globin and the sgRNA targeting *HBB* should avoid the excessive reduction of β-like globin chains, a potential issue of this strategy is the possibility to generate a β-thalassemic phenotype in the absence of a sufficient amount of transgene-derived AS3-globin to compensate β^S-downregulation.

SCD HSPCs were transduced with the LV AS3m.C, transfected with Cas9-GFP protein, and then *in vitro* differentiated into mature RBCs (Figure 6A). Erythroid cultures obtained from SCD or HD HSPCs transfected with Cas9 ribonucleoprotein (RNP) complexes containing gR-C were used as β-thalassemia-like control cells (Figure 6A). Mature RBCs derived from SCD or HD HSPCs treated with gR-C-RNP displayed a strong reduction in the HbS and HbA content, respectively, and an increased α chain/non-α chain ratio in comparison to untreated controls (Figure 6B). On the contrary, in RBCs derived from *HBB*-edited, LV AS3m.C-transduced SCD HSPCs, α-chain/non-α chain ratios remained largely unchanged (1.08 ± 0.04; n = 14) compared to untreated controls and mock-transfected, LV AS3m.C-treated samples (1.05 ± 0.03; n = 15)

The erythroid differentiation of edited HSPCs cells treated with LV AS3m.C was not impaired. Indeed, the expression of surface markers identifying the different erythroid populations (CD36, CD71, CD235A, CD49d, and Band3) and the frequency of enucleated cells were similar in control and treated samples all along the differentiation (Figures 7A–7E; Figure S7A). On the contrary, in β-thalassemia-like cells erythroid differentiation was delayed as well as RBC enucleation (Figures 7A–7E).

Furthermore, we acquired images from *in vitro*-differentiated RBCs derived from SCD HSPCs treated with LV AS3m.C to evaluate several morphological and physical parameters in a quantitative manner (Figure 6A). β-Thalassemia-like RBCs were characterized by a reduced dry mass compared to mock-treated control samples, due to the lower Hb content (Figure 7F; Figure S7B). Surface, perimeter, and ellipticity parameters were altered in β-thalassemia-like RBCs (Figures 7G–7I; Figures S7C–S7E), reflecting the anisocytosis and poikilocytosis characterizing β-thalassemic RBCs.[45,46] In RBCs derived from LV AS3m.C-treated SCD HSPCs harboring ∼42% of edited *HBB* alleles, only a small percentage of cells showed reduced dry mass, surface, and perimeter (6.2% ± 2.3%, 5.4% ± 3.6% and 6.5% ± 3.7%; n = 2, respectively) in comparison to RBCs obtained from mock-transfected LV AS3m.C HSPCs (Figures 7F–7H; Figures S7B and S7D), while ellipticity was overall unaffected (Figure 7I; Figure S7E). These frequencies were modestly increased in RBCs derived from SCD HSPCs harboring 63% of edited alleles (10.1% for dry mass, 13.4% for surface, and 10.2% for perimeter).

Finally, editing of *HBG* promoters did not impact the differentiation and enucleation of LV AS3m.13bpdel-transduced SCD HSPCs (Figures S8B–S8E). α-Chain/non-α chain ratios, surface, dry mass, perimeter, and ellipticity were similar in RBCs derived from edited LV AS3m.13bpdel-transduced HSPCs and control samples (Figures S8A and S8F–S8I).

In conclusion, these analyses showed that erythroid differentiation of SCD HSPCs edited using bifunctional LVs and Cas9 transfection is largely unaltered.

DISCUSSION

LVs expressing a β-globin transgene to compensate β-globin deficiency in β-thalassemia, or to inhibit Hb polymerization in SCD, have shown promising clinical outcomes[7,11,47]. However, to be effective, gene addition strategies require the sustained engraftment of highly transduced HSCs.[8] This could increase the genotoxic risk particularly in SCD patients who have an increased probability of developing hematological malignancies compared to the general population.[48,49] While promising approaches aimed at improving LV-derived transgene expression have been investigated,[50] reaching therapeutic globin expression with a low VCN is still challenging, as LVs cannot accommodate the entire β-globin locus control region (βLCR) responsible for high-level expression of the β-like globin genes.

Interestingly, clinical observations in a compound β^0/β^S heterozygous SCD patient indicate that β-globin deficiency was associated with amelioration of the disease phenotype despite the relatively low gene marking in engrafted HSCs.[8] Furthermore, a mild disease

Figure 4. Testing of LV AS3m.13bpdel and LV AS3m.BCL11A in SCD HSPCs

(A) Schematic representation of the protocol used to transduce and transfect SCD HSPCs. 24 h after thawing, HSPCs were transduced with LV AS3m.13bpdel and LV AS3m.BCL11A, and after 48 h cells were transfected with the Cas9-GFP protein and differentiated into mature RBCs following a 21-day differentiation protocol. (B) Correlation between VCN and indel frequency in cells treated with LVs AS3m.BCL11A (one mobilized SCD donor) and AS3m.13bpdel (two mobilized SCD donors). R^2 and line-of-best-fit equation are indicated. (C) Deep-sequencing analyses of the 13bpdel off-target in mature erythroblasts derived from adult SCD HSPCs treated with LV AS3m.13bpdel. Transduced and mock-transfected SCD cells (Ctr) are indicated in red and edited samples (AS3m.13bpdel) in black. (D) GUIDE-seq analysis of gR-BCL11A in 293T cells. The protospacer targeted by gR-BCL11A and the PAMs are shown in the first line. Off-targets and their mismatches with the on-target (highlighted in color), sequencing read counts, and chromosomal position are reported. (E) Relative expression of *HBG* mRNA normalized to α-globin in untreated SCD cells (Ctr) (n = 5) and cells treated with LV AS3m.13bpdel (n = 14, 2 SCD donors). ***p < 0.001 (unpaired t test). Horizontal lines indicate median and first and third quartiles. (F) Representative flow cytometry analysis of F cells in RBCs derived from untreated (Ctr UT; light blue), and LV AS3m.13bpdel-treated SCD HSPCs mock transfected (medium blue) or transfected with Cas9-GFP (dark blue) (two mobilized SCD donors). (G) Correlation between VCN and percentage of HbS and HbAS3 (determined by CE-HPLC) in cells derived from mock-transfected (orange and light blue) and Cas9-transfected (red and dark blue) SCD HSPCs transduced with LV AS3m.13bpdel (two mobilized SCD donors). We plotted the percentage of HbS or HbAS3+HbF over the total Hbs. R^2 and line-of-best-fit equation are indicated. Dashed lines indicate the VCN required to achieve equal amounts of HbS and HbAS3. (H) Correlation between indel frequency and percentage of HbS and HbAS3 (determined by CE-HPLC) in cells derived from Cas9-transfected SCD HSPCs transduced with LV AS3m.13bpdel (two mobilized SCD donors). R^2 and line-of-best-fit equation are indicated.

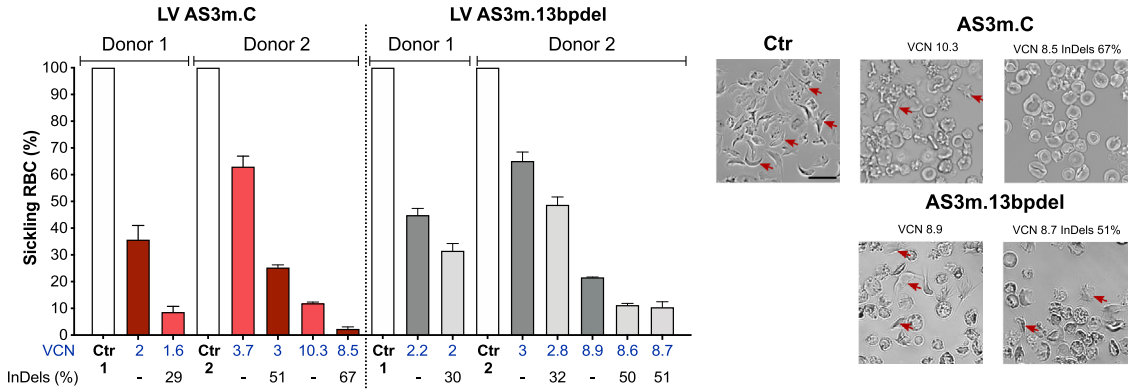

Figure 5. The bifunctional LVs AS3m.C and AS3m.13bpdel reduce RBC sickling

In vitro sickling assay measuring the proportion of sickled RBCs under hypoxic conditions (0% O_2). We reported the percentage of sickling RBCs (left panel) and representative photomicrographs of RBCs derived from control (Ctr), LVs AS3m.C and AS3m.13bpdel samples that were either mock transfected or transfected with Cas9-GFP (right panel; 2 SCD donors). Arrows indicate sickling cells. Data are expressed as mean ± SEM. Scale bar, 20 μm (upper left).

phenotype is observed in SCD and β-thalassemia patients harboring HPFH mutations.[19,51,52] These clinical outcomes support the rationale of the design of gene therapy approaches that combine the expression of an anti-sickling β-globin transgene with editing strategies aimed to either reduce the β^S-globin expression or to increase the γ-globin content to counteract HbS polymerization in SCD or to increase Hb content in β-thalassemia.

We designed LVs simultaneously driving the expression of a β-globin chain carrying three anti-sickling amino acids,[13] and a sgRNA either to introduce frameshift mutations in the *HBB* gene (LV AS3m.C) or to reactivate HbF expression by disrupting the BCL11A binding site in the γ-globin promoters (LV AS3m.13bpdel)[5] or by downregulating BCL11A expression (LV AS3m.BCL11A).[5]

The editing efficiency at the on-target loci was positively correlated with the number of integrated LV copies in HUDEP-2 cells and SCD primary HSPCs, demonstrating the efficient LV-derived sgRNA expression and the formation of the functional CRISPR-Cas9 RNP complexes in transfected cells. These data are in line with combinatorial systems based on the stable LV-mediated delivery of sgRNAs coupled with transient transfection of Cas9 mRNA in human HD HSPCs to downregulate the expression of cell surface proteins.[53] Importantly, we achieved high editing efficiencies using Cas9 protein delivery that we previously demonstrated to be less toxic and more efficient than mRNA delivery in primary HSPCs.[43] A recent report showed that precomplexing of Cas9 protein with a non-targeting sgRNA was required to achieve high genome editing frequency using LV-delivered sgRNAs.[54] Interestingly, our system was already efficient by transfecting Cas9 protein alone, and the editing efficiency was not further increased by complexing the Cas9 with a nontargeting sgRNA (data not shown). Importantly, we applied this technology to develop a gene therapy approach for β-hemoglobinopathies by combining the efficient LV-based delivery of sgRNAs with the expression of a therapeutic β-globin transgene.

The delivery of Cas9 protein in clinically relevant SCD HSPCs transduced with LV AS3m.C resulted in robust downregulation of *HBB* expression at both the mRNA and protein levels. Of note, introduction of silent mutations in the AS3 sequence prevented undesired editing and inactivation of the transgene. The increased availability of α-globin chains caused by β-globin downregulation favored the formation of AS3-containing Hb tetramers, thus increasing the total anti-sickling Hb content in RBCs derived from edited HSPCs, as compared to RBCs obtained from control HSPCs harboring a similar number of LV copies. In a parallel approach, the editing of the γ-globin promoters in SCD HSPCs transduced with LV AS3m.13bpdel increased the total content of anti-sickling Hb tetramers by inducing the expression of both Gγ- and Aγ-globins. As previously reported,[20,23,55,56] editing of the −115 region of the *HBG* promoters disrupts the *BCL11A* binding site and evicts BCL11A, allowing the recruitment of the NF-Y transcriptional activator at the −86 region and γ-globin reactivation. The sgRNAs targeting the *HBB* gene or the *HBG* promoters showed minimal off-target activity as detected by GUIDE-seq and targeted NGS sequencing of the potential off-targets. However, although GUIDE-seq was identified as the best performing assay for *ex vivo* therapeutics,[57–59] it has a limited sensitivity (0.1%) and therefore could fail to detect off-target events that occur at a low frequency but can still potentially lead to deleterious outcomes (e.g., clonal expansion and malignant neoplasms). More sensitive assays to assess the potential CRISPR-Cas9-associated genotoxic risk should be developed in particular for clinical applications aimed to modify hundreds of millions of cells.

Surprisingly, LV AS3m.BCL11A showed poor transduction and editing efficiencies in the *BCL11A* erythroid-specific enhancer in SCD HSPCs. We have not clarified the mechanisms of poor transduction by LV AS3m.BCL11A. In cell lines, we have not observed any significant difference in titer and infectivity between LV AS3m.BCL11A and the other vectors, although the LV harboring the sgRNA targeting the

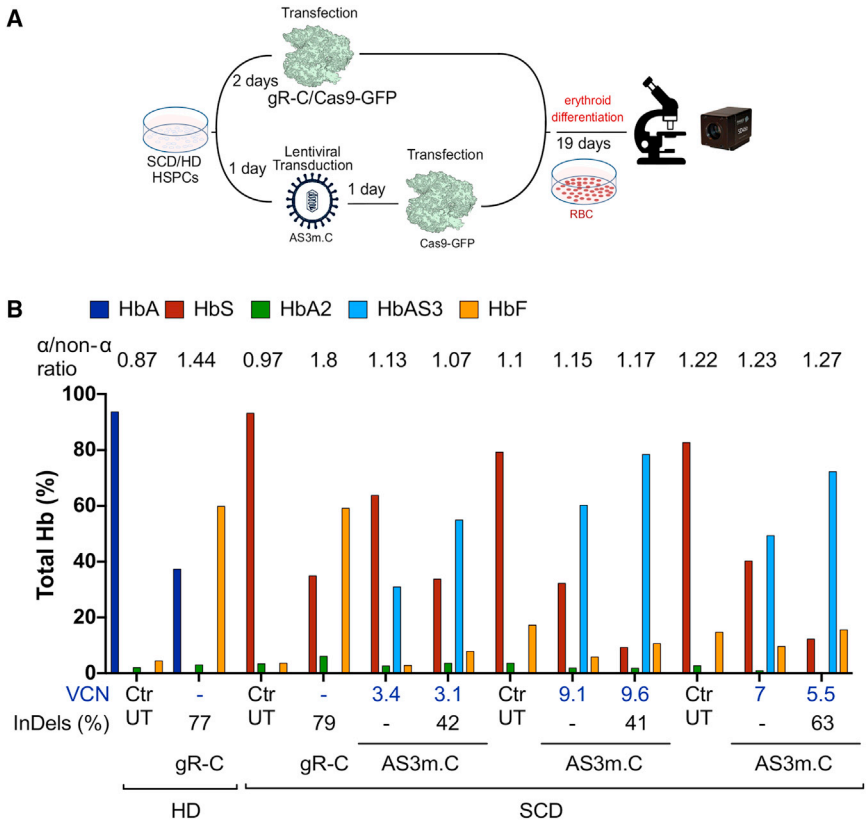

Figure 6. The bifunctional LV downregulating HbS does not generate a β-thalassemic phenotype

(A) Schematic representation of the protocol used to evaluate erythroid differentiation and RBC parameters. We transduced SCD/HD HSPCs with LV AS3m.C and transfected them with Cas9 protein. As controls, we transfected SCD/HD HSPCs with RNPs containing gR-C. Images of *in vitro*-cultured RBCs were taken using the Phasics SID4-HR GE camera. The BIO-Data interface software was used to analyze RBC images. (B) CE-HPLC quantification of Hb tetramers in untreated HD and SCD cells (Ctr UT), gR-C-treated HD and SCD cells (gR-C), and LV AS3m.C-treated SCD HSPCs that were mock transfected ("–") or transfected with Cas9-GFP protein. We plotted the percentage of each Hb type over the total Hb tetramers. VCN values are reported in blue and indels in black below the graph. The α-globin/non-α-globin ratio (determined by RP-HPLC) is reported on top of the histograms.

BCL11A enhancer tends to have a lower infectivity that could impact the efficiency of transduction of primary HSPCs. In our previous study, we also compared LVs with similar titer and infectivity (as determined in cell lines) and observed, for some of these vectors, a low transduction of HSPCs, likely related to specific sequences that are detrimental to the vector performance in primary cells.[43] Furthermore, bi-allelic disruption of this enhancer is required to achieve HbF reactivation, and the selected sgRNA targeting *BCL11A*[26] showed numerous potential off-target sites. For these reasons, we decided not to further pursue this approach. The selection of a more efficient and specific sgRNA disrupting critical regions in the *BCL11A* enhancer will allow us to ameliorate this therapeutic approach in future experiments.

Interestingly, the high content of anti-sickling hemoglobins observed with both LV AS3m.C and LV AS3m.13bpdel resulted in reduced HbS levels, Hb polymerization, and frequency of sickled RBCs compared to the conventional gene addition approach. Importantly, compared to a LV expressing only the anti-sickling transgene, our combined approach requires a lower VCN to achieve a therapeutic effect, thus reducing the potential genotoxicity risk associated with LV integration. In particular, we achieved similar amounts of HbS and anti-sickling hemoglobins (resembling the Hb profile of an asymptomatic heterozygous SCD carrier) with a VCN of ∼5.5 using the conventional gene addition strategy, and a VCN of ∼2.2 and ∼3.7 (associated with 30%–35% of edited *HBB* or *HBG* genes) using LV AS3m.C and LV AS3m.13bpdel, respectively. As a higher VCN was required to reach a similar editing frequency for LV AS3m.13bpdel compared to LV AS3m.C, we hypothesize that the difference in the extent of the correction of the disease phenotype between these two approaches is due to the higher editing efficiency of the gR-C compared to the sgRNA targeting the *HBG* promoters. Alternative sgRNAs targeting HbF inhibitory sequences[23,60] could be tested in future studies to further enhance γ-globin reactivation with a lower VCN.

Importantly, we used flow cytometry and quantitative phase imaging to evaluate erythroid differentiation of edited HSPCs and quantify at a single-cell level morphological and physical parameters of *in vitro*-differentiated RBCs. This study is fundamental to demonstrate the safety of HSC-based treatments for β-hemoglobinopathies. β-Thalassemic erythroid cells showed delayed differentiation and enucleation, imbalance in the α-chain/non-α chain ratio, α-precipitates, anisocytosis, and poikilocytosis. Editing of the *HBB* gene or the γ-globin promoters in HSPCs did not negatively impact their differentiation and enucleation rate, allowing the production of mature RBCs with Hb content and morphological parameters largely similar to untreated controls. In particular, in erythroid cells derived from *HBB*-edited HSPCs, AS3-globin chain expression was sufficient to compensate for the lack of β^S-globin expression in the vast majority of RBCs. In fact, only a small percentage of RBCs (∼5%–10%) displayed a β-thalassemic-like phenotype. We can speculate that a small fraction of poorly transduced HSPCs harboring bi-allelic disruption of the *HBB* gene give rise to this RBC subpopulation producing AS3 levels, which are insufficient to compensate β^S downregulation. Importantly, preclinical and clinical data indicate that in allotransplanted or gene therapy-treated β-thalassemia subjects, β-thalassemic cells are counterselected *in vivo* because the erythroid precursors undergo apoptosis, and mature RBCs have a

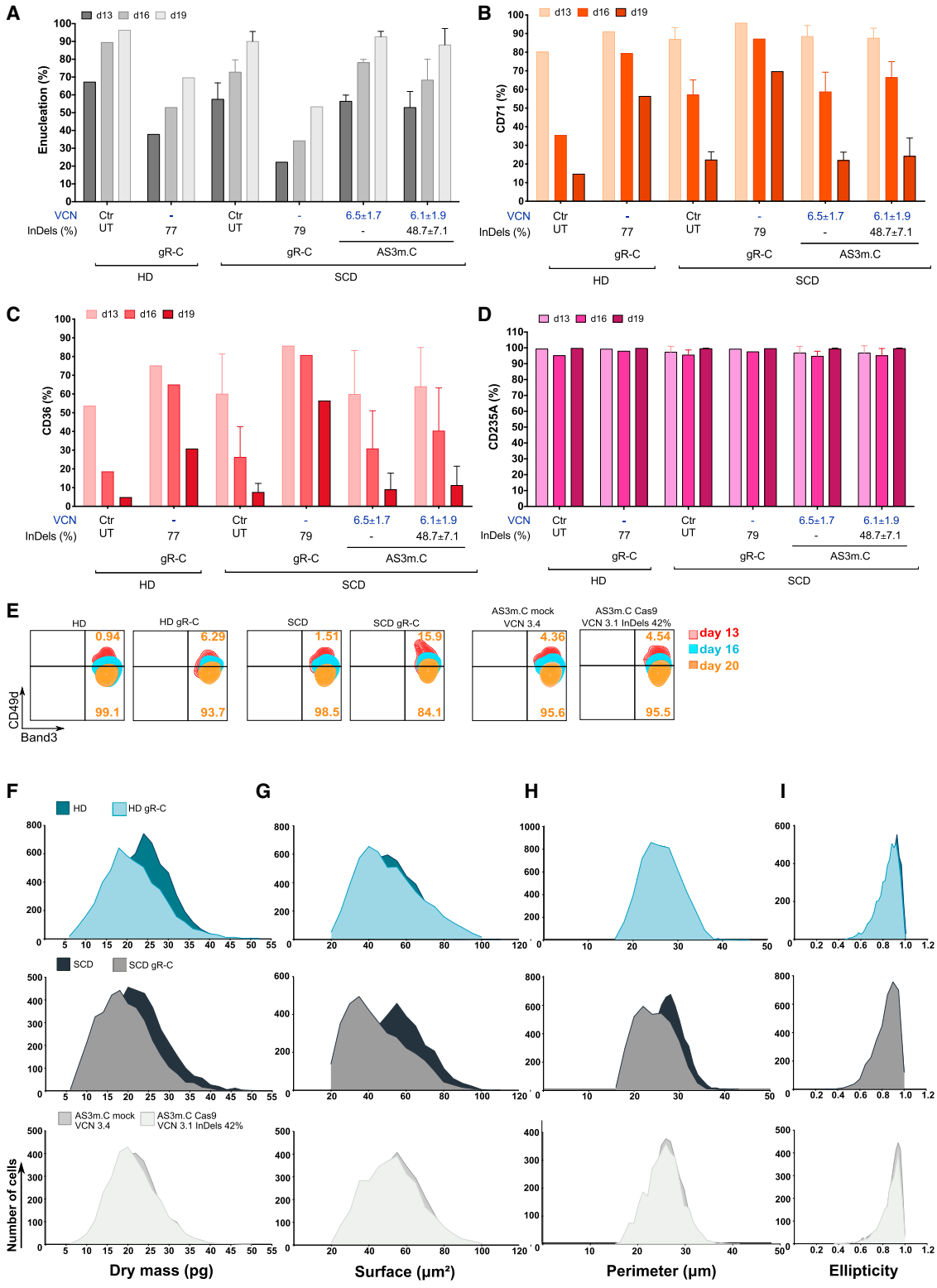

(legend on next page)

shorter lifespan compared to HD or corrected cells.[5,11,61] Furthermore, we do not expect that such a low frequency of β-thalassemic RBCs will impact the correction of the SCD phenotype *in vivo*.

Other therapeutic strategies for SCD aim at reverting the SCD mutation by cleaving the sickle *HBB* gene using the CRISPR-Cas9 system and inserting through the HDR pathway a donor template containing the WT *HBB* sequence that is either provided as a single-strand oligonucleotide or delivered by a viral vector.[14,62,63] More recently, we proposed a combined treatment for β-thalassemia based on the insertion of the AS3 transgene in the α-globin (*HBA*) locus to simultaneously express the therapeutic β-globin while reducing *HBA* expression levels[36] and α-globin precipitates. However, although more promising than the standard gene addition strategy, these approaches currently suffer from poor HDR efficiency in HSCs. On the contrary, our combined approach is likely more prone to produce the desired genome modification, as it relies on the NHEJ pathway, known to be preferentially active and more efficient in HSCs compared to HDR.[64–67] Moreover, in SCD, failed HDR-mediated gene correction likely results in the NHEJ-mediated *HBB* gene disruption, which could likely not be compensated by the residual endogenous β-like globin chains, thus potentially generating a β-thalassemic phenotype.[68] The generation of a β-thalassemia phenotype was observed only in a small fraction of RBCs using our combined strategy, as the same LV is co-expressing the sgRNA targeting *HBB* and the therapeutic AS3 chain that compensates for the knockdown of the endogenous *HBB*.

Ongoing trials for β-hemoglobinopathies using a genome editing strategy efficiently targeting the *BCL11A* enhancer showed early promising results.[28] However, HbF reactivation and therapeutic benefit were modest when editing occurred at low efficiency.[40] Furthermore, as reported in trials based on LV gene addition approaches, some patients did not attain normal levels of total Hb, and in SCD subjects HbS levels were not always decreased to the values observed in an asymptomatic heterozygous SCD carrier, suggesting the persistence of a subset of non-corrected RBCs.[69]

Our strategies combine two gene therapy platforms currently under evaluation in experimental clinical trials for β-hemoglobinopathies, potentially improving the efficacy of gene therapy to treat SCD and even β-thalassemia when AS3 expression is combined with HbF reactivation. Notably, in our strategies bi-allelic editing is likely not required when targeting either the sickle β-globin gene or the *HBG* promoters. However, there are some concerns related to the risks of combining LV and CRISPR-Cas9 approaches, which can both lead to potential deleterious DNA mutagenesis and DNA damage response. Although our study suggests that the treatment of patient HSPCs with both LV and Cas9 did not affect progenitor growth and differentiation, predictive assays, such as xenotransplantation in immunodeficient mouse models, are required to demonstrate the safety of the proposed approaches in repopulating stem cells and their progeny.

Finally, bifunctional LVs can have a wider range of potential applications in this field. In fact, by simply modifying the sgRNA sequence, the bifunctional LVs could be exploited to develop different therapeutic approaches for β-hemoglobinopathies (e.g., sickle β-globin or *BCL11A* downregulation;[26] inactivation of *HBG* inhibitory sequences;[20,23] insertion of *HBG* activating sequences[70,71]) by using a variety of editing tools (e.g., Cas9 nucleases, base editors, epigenome editors, and prime editors[72–74]).

More generally, the combination of gene addition and genome editing strategies has the potential to simultaneously induce the expression of therapeutic proteins and downregulate disease-causing genes. By way of example, we envision that this versatile technology can allow the development of therapeutic strategies for the treatment of autosomal dominant disorders, which requires the downregulation of the dominant allele. As it is difficult to achieve targeted downregulation of the mutant gene without impairing the expression of the WT allele, our strategy could allow the disruption of the endogenous genes, and simultaneously the LV-derived expression of a non-targeted WT allele (i.e., harboring silent mutations, which impair sgRNA binding and transgene disruption).

MATERIALS AND METHODS

LV production and titration

For LV production, the expression cassette consisting of DNase I hypersensitive sites HS2 (genomic coordinates [hg38]: chr11:5280255–5281665) and HS3 (genomic coordinates [hg38]: chr11:5284251–5285452) of the βLCR,[75] and a *HBB* mini-gene extending from −265 bp upstream of the transcriptional start site to +300 bp downstream of the poly(A) addition site (genomic coordinates [hg38]: chr11:5225174–5227336) with a short version of intron 2 (genomic coordinates [hg38]: chr11:5203703–5204295) was cloned into a

Figure 7. Erythroid differentiation and RBC parameters were not impaired in cells derived from LV AS3m.C-transduced, edited SCD HSPCs

(A–E) Flow cytometry analysis of the enucleation rate and of the early (CD71, CD36, and CD49d) and late (CD235A and Band3) erythroid markers at day 13, 16, and 19 or 20 of erythroid differentiation of untreated HD (n = 1) and SCD (n = 3) cells (Ctr UT), gR-C-treated HD (n = 1) and SCD (n = 1) cells (gR-C), and LV AS3m.C-treated SCD HSPCs that were mock transfected or transfected with Cas9-GFP protein (n = 3). VCN and indel values are reported below the graph as mean ± SEM. (A–D) Data are expressed as mean ± SEM. (A) Enucleation rate measured using DRAQ5 nuclear staining. (B–D) Proportion of $CD71^+$, $CD36^+$, and $CD235A^+$ cells during erythroid differentiation. (E) Expression of CD49d and Band3 during the erythroid differentiation. During terminal erythroid differentiation, cells lose CD49d expression. (F–I) RBC parameters extracted using the BIO-Data software. RBCs were obtained after 19 days of differentiation from SCD HSPCs transduced with LV AS3m.C and either mock or Cas9 transfected. As controls, we used RBCs obtained from SCD/HD HSPCs transfected with RNPs containing gR-C For each population; data were normalized to the total number of RBCs and are reported as overlaid histograms. Darker colors represent controls and lighter colors edited samples. From top to bottom: control HD RBCs compared with HD RBCs derived from HSPCs treated with gR-C; control SCD RBCs compared with SCD RBCs derived from HSPCs treated with gR-C; control SCD RBCs derived from HSPCs transduced with LV AS3m.C and mock transfected compared to RBCs derived from HSPCs transduced with LV AS3m.C and transfected with Cas9 protein. (F) Dry mass (pg). (G) Surface (μm^2). (H) Perimeter (μm). (I) Ellipticity.

pCCL LV backbone to generate the pCCL.β-globin plasmid. The mutations determining three anti-sickling amino acid substitutions (G16D, E22A, and T87Q)[13] were introduced in the pCCL.β-globin plasmid by *in vitro* site-directed mutagenesis to obtain the pCCL.AS3 plasmid. Silent mutations were inserted in the 19-bp AS3 transgene sequence recognized by gR-C to generate the pCCL.AS3m plasmid. To insert silent mutations, we used synonymous codons from *HBB*, *HBD*, *HBG1*, and *HBG2* genes.

Synthetic oligonucleotides (Integrated DNA Technologies) containing the sgRNA expression cassette (with the optimized sgRNA scaffold[35]) were inserted in pCCL.AS3m, generating the transfer vectors (pCCL.AS3m.gRs) for the LV production.

Third-generation LVs were produced by calcium phosphate transient transfection of HEK293T cells with the transfer vector (pCCL.AS3m or pCCL.AS3m.gRs), the packaging plasmid pKLg/p.RRE, the Rev-encoding plasmid pK.REV, and the vesicular stomatitis virus glycoprotein G (VSV-G) envelope-encoding plasmid pK.G. The physical titer of vector preparations was measured using the HIV-1 Gag p24 antigen immunocapture assay kit (PerkinElmer, Waltham, MA, USA) and expressed as p24 ng/mL. The viral infectious titer was calculated by transducing HCT116 cells with serial vector dilutions, as previously described.[76] VCN per diploid genome was calculated to determine the viral infectious titer, expressed as TU/mL. Viral infectivity was calculated as the ratio between infectious and physical titers (TU/ng p24).

HSPC transduction and transfection

We isolated cord blood $CD34^+$ HSPCs and adult granulocyte colony-stimulating factor (G-CSF)-mobilized HSPCs from healthy donors. Human adult $CD34^+$ HSPCs were isolated from the blood of SCD patients either after plerixafor mobilization (ClinicalTrials.gov: NCT02212535, Necker Hospital, Paris, France) or after erythrocytapheresis. Written informed consent was obtained from all of the subjects. All experiments were performed in accordance with the Declaration of Helsinki. The study was approved by the Regional Investigational Review Board (reference: DC 2014-2272, CPP Ile-de-France II "Hôpital Necker-Enfants malades"). HSPCs were purified by immunomagnetic selection with autoMACS (Miltenyi Biotec) after immunostaining with a CD34 MicroBead kit (Miltenyi Biotec). $CD34^+$ cells were cultured (10^6 cells/mL) 24 h before transduction in X-VIVO 20 supplemented with penicillin/streptomycin (Gibco, Carlsbad, CA, USA), StemRegenin1 (SR1) at 250 nM (STEMCELL Technologies), and the following recombinant human cytokines (PeproTech): 300 ng/mL stem cell factor (SCF), 300 ng/mL Flt-3L, 100 ng/mL thyroperoxidase (TPO), and 60 ng/mL interleukin (IL)-3 ("expansion medium").

Two hours before LV transduction, $CD34^+$ cells were plated in RetroNectin-coated plates (10 μg/cm^2, Takara Bio, Kusatsu, Japan) at 3×10^6 cells/mL in the expansion medium supplemented with 16,16-dimethyl-prostaglandin E_2 (PGE2) (10 μM PGE2; Cayman Chemical).[77,78] Cells were then transduced for 24 h in the expansion medium supplemented with protamine sulfate (4 μg/mL, Sigma-Aldrich, St. Louis, MO, USA or APP Pharmaceuticals, Schaumburg, IL, USA), PGE2, and LentiBOOST (Sirion Biotech[69]). After expansion of $CD34^+$ cells for 48 h, 100,000 cells were transfected with 15 μg of Cas9-GFP protein (provided by Dr. De Cian) by using the P3 Primary Cell 4D-Nucleofector X kit S (Lonza) and the AMAXA 4D CA137 program (Lonza). After transfection, cells were plated at a concentration of 50,000 cells/mL in the erythroid differentiation medium.

Erythroid differentiation of HSPCs

After transfection, HSPCs were differentiated into mature RBCs using a three-phase protocol.[44] From day 0 to day 6, cells were grown in a basal erythroid medium[6] supplemented with 10^{-6} M hydrocortisone (Sigma), 100 ng/mL SCF (PeproTech), 5 ng/mL IL-3 (PeproTech), and 3 IU/mL erythropoietin (EPO) (Eprex, Janssen-Cilag). From day 6 to day 9, cells were cultured onto a layer of murine stromal MS-5 cells in the basal erythroid medium supplemented only with 3 IU/mL EPO. Finally, from day 9 to day 20, cells were cultured on a layer of MS-5 cells in the basal erythroid medium without any cytokines. Erythroid differentiation and enucleation rate were monitored by flow cytometry analysis.

RP- and CE-HPLC analysis

For HPLC analyses, HUDEP-2 cells were collected at day 9 of erythroid differentiation, whereas *in vitro*-differentiated RBCs were collected at day 20 of erythroid differentiation.

RP-HPLC analyses were performed using a Nexera X2 SIL-30AC chromatograph (Shimadzu) and the Lc Solution software. Globin chains were separated by HPLC using a 250 × 4.6 mm, 3.6-μm Aeris Widepore column (Phenomenex). Samples were eluted with a gradient mixture of solution A (water/acetonitrile/trifluoroacetic acid, 95:5:0.1) and solution B (water/acetonitrile/trifluoroacetic acid, 5:95:0.1). The absorbance was measured at 220 nm.

CA-HPLC analyses were performed using a Nexera X2 SIL-30AC chromatograph (Shimadzu) and the Lc Solution software. Hemoglobin tetramers were separated by HPLC using a two cation-exchange column (PolyCAT A, PolyLC, Columbia, MD, USA). Samples were eluted with a gradient mixture of solution A (20 mM bis-Tris, 2 mM KCN [pH 6.5]) and solution B (20 mM bis-Tris, 2 mM KCN, 250 mM NaCl [pH 6.8]). The absorbance was measured at 415 nm.

Sickling assay

In vitro-differentiated RBCs (day 19–20 of differentiation) derived from treated and control SCD HSPCs were exposed to an oxygen-deprived atmosphere (0% O_2) and the time course of sickling was monitored in real time by video microscopy for 1 h, capturing images every 20 min using the Axio Observer Z1 microscope (Zeiss) and a ×40 objective. At 0% O_2, around 400 cells per condition were counted and processed with ImageJ to determine the percentage of sickled RBCs in the total cell population.

Quantitative phase image microscopy of RBCs

50,000 to 100,00 *in vitro*-differentiated RBCs were centrifuged at 1,500 rpm for 5 min, resuspended in 50 or 700 μL of PBS 0.5% BSA, and placed in a μ-Slide with 15 or 8 wells (ibidi), respectively. We used the SID4 HR GE camera (Phasics, Saint-Aubin, France) with an inverted microscope (Eclispe Ti-E, Nikon) to obtain quantitative phase images of label-free RBCs.[79] Images were taken using a ×40/0.60 objective. The BIO-Data R&D software (version 2.7.1.46) was used to perform a segmentation procedure to isolate each RBC from an image. We analyzed only enucleated RBCs, discarding cells with a surface density (dry mass/surface) higher than 0.55 pg/μm^2. For each RBC, we evaluated dry mass (pg), surface (μm^2), perimeter (μm), and ellipticity.[80]

Statistical analysis

Data were analyzed with GraphPad Prism software (version 7.0) and expressed as mean ± standard error of the mean (SEM), unless stated otherwise. Parametric tests (Student's t test, unpaired t tests, two- or pne-way ANOVA test, and Sidak's, Dunnett's, and Tukey's multiple comparisons test) were used according to datasets. The threshold for statistical significance was set to $p < 0.05$. Linear or non-linear regression analyses were performed to assess the correlation between frequency of genome editing and VCN or between frequency of genome editing or VCN and Hb expression.

SUPPLEMENTAL INFORMATION

Supplemental information can be found online at https://doi.org/10.1016/j.ymthe.2021.08.019.

ACKNOWLEDGMENTS

This work was supported by State funding from the Agence Nationale de la Recherche under "Investissements d'avenir" program (ANR-10-IAHU-01), the Paris Ile de France Region under "DIM Thérapie génique" initiative, the Société d'Accélération du Transfert de Technologies-SATT IDF Innov, the Fondation Maladies Rare, and the Sanofi Innovation Award. We thank Sylvie Fabrega (Plateforme Vecteurs Viraux et Transfert de Gènes, SFR Necker, US 24, UMS 3633, 75014 Paris, France) for the LV production

AUTHOR CONTRIBUTIONS

S.R. designed and performed experiments, analyzed data, and wrote the paper; A.C., T.F., G.F., M.B., A. Casini, and G.M. performed experiments and analyzed data; N.O. and S.A. analyzed quantitative phase microscopy, C.M. analyzed off-target NGS data; A.D.C. provided reagents; J.-P.C., M.C., A. Cereseto, W.E.N., M.A., and B.W. contributed to the design of the experimental strategy; V.M. conceived the study, designed and performed experiments, analyzed data, and wrote the paper; A.M. conceived the study, designed experiments, analyzed data, and wrote the paper.

DECLARATION OF INTERESTS

V.M. and A.M. are the inventors of two patents describing this gene addition/genome editing platform (WO/2018/220211, "Viral vectors combining gene therapy and genome editing approaches for gene therapy of genetic disorders"; WO/2018/220210, "Recombinant lentiviral vector for stem cell-based gene therapy of sickle cell disorder). The remaining authors declare no competing interests.

REFERENCES

1. Cavazzana, M., Antoniani, C., and Miccio, A. (2017). Gene therapy for β-hemoglobinopathies. Mol. Ther. *25*, 1142–1154.
2. Ngo, S., Bartolucci, P., Lobo, D., Mekontso-Dessap, A., Gellen-Dautremer, J., Noizat-Pirenne, F., Audard, V., Godeau, B., Galacteros, F., Habibi, A., and (. (2014). Causes of death in sickle cell disease adult patients: Old and new trends. Blood *124*, 2715.
3. Sadelain, M., Boulad, F., Galanello, R., Giardina, P., Locatelli, F., Maggio, A., Rivella, S., Riviere, I., and Tisdale, J. (2007). Therapeutic options for patients with severe β-thalassemia: The need for globin gene therapy. Hum. Gene Ther. *18*, 1–9.
4. Besse, K., Maiers, M., Confer, D., and Albrecht, M. (2016). On modeling human leukocyte antigen-identical sibling match probability for allogeneic hematopoietic cell transplantation: Estimating the need for an unrelated donor source. Biol. Blood Marrow Transplant. *22*, 410–417.
5. Miccio, A., Cesari, R., Lotti, F., Rossi, C., Sanvito, F., Ponzoni, M., Routledge, S.J., Chow, C.M., Antoniou, M.N., and Ferrari, G. (2008). In vivo selection of genetically modified erythroblastic progenitors leads to long-term correction of β-thalassemia. Proc. Natl. Acad. Sci. USA *105*, 10547–10552.
6. Weber, L., Poletti, V., Magrin, E., Antoniani, C., Martin, S., Bayard, C., Sadek, H., Felix, T., Meneghini, V., Antoniou, M.N., et al. (2018). An optimized lentiviral vector efficiently corrects the human sickle cell disease phenotype. Mol. Ther. Methods Clin. Dev. *10*, 268–280.
7. Ribeil, J.-A., Hacein-Bey-Abina, S., Payen, E., Magnani, A., Semeraro, M., Magrin, E., Caccavelli, L., Neven, B., Bourget, P., El Nemer, W., et al. (2017). Gene therapy in a patient with sickle cell disease. N. Engl. J. Med. *376*, 848–855.
8. Magrin, E., Miccio, A., and Cavazzana, M. (2019). Lentiviral and genome-editing strategies for the treatment of β-hemoglobinopathies. Blood *134*, 1203–1213.
9. Cavazzana-Calvo, M., Payen, E., Negre, O., Wang, G., Hehir, K., Fusil, F., Down, J., Denaro, M., Brady, T., Westerman, K., et al. (2010). Transfusion independence and *HMGA2* activation after gene therapy of human β-thalassaemia. Nature *467*, 318–322.
10. Kaiser, J. (2021). Gene therapy trials for sickle cell disease halted after two patients develop cancer, https://www.sciencemag.org/news/2021/02/gene-therapy-trials-sickle-cell-disease-halted-after-two-patients-develop-cancer.
11. Marktel, S., Scaramuzza, S., Cicalese, M.P., Giglio, F., Galimberti, S., Lidonnici, M.R., Calbi, V., Assanelli, A., Bernardo, M.E., Rossi, C., et al. (2019). Intrabone hematopoietic stem cell gene therapy for adult and pediatric patients affected by transfusion-dependent β-thalassemia. Nat. Med. *25*, 234–241.
12. Miccio, A., Poletti, V., Tiboni, F., Rossi, C., Antonelli, A., Mavilio, F., and Ferrari, G. (2011). The GATA1-HS2 enhancer allows persistent and position-independent expression of a β-globin transgene. PLoS ONE *6*, e27955.
13. Levasseur, D.N., Ryan, T.M., Reilly, M.P., McCune, S.L., Asakura, T., and Townes, T.M. (2004). A recombinant human hemoglobin with anti-sickling properties greater than fetal hemoglobin. J. Biol. Chem. *279*, 27518–27524.
14. Dever, D.P., Bak, R.O., Reinisch, A., Camarena, J., Washington, G., Nicolas, C.E., Pavel-Dinu, M., Saxena, N., Wilkens, A.B., Mantri, S., et al. (2016). CRISPR/Cas9 β-globin gene targeting in human haematopoietic stem cells. Nature *539*, 384–389.
15. Wilkinson, A.C., Dever, D.P., Baik, R., Camarena, J., Hsu, I., Charlesworth, C.T., Morita, C., Nakauchi, H., and Porteus, M.H. (2021). Cas9-AAV6 gene correction of beta-globin in autologous HSCs improves sickle cell disease erythropoiesis in mice. Nat. Commun. *12*, 686.
16. Park, S.H., Lee, C.M., Dever, D.P., Davis, T.H., Camarena, J., Srifa, W., Zhang, Y., Paikari, A., Chang, A.K., Porteus, M.H., et al. (2019). Highly efficient editing of the β-globin gene in patient-derived hematopoietic stem and progenitor cells to treat sickle cell disease. Nucleic Acids Res. *47*, 7955–7972.
17. Genovese, P., Schiroli, G., Escobar, G., Tomaso, T.D., Firrito, C., Calabria, A., Moi, D., Mazzieri, R., Bonini, C., Holmes, M.C., et al. (2014). Targeted genome editing in human repopulating haematopoietic stem cells. Nature *510*, 235–240.

18. Magis, W., DeWitt, M.A., Wyman, S.K., et al. (2019). High-level correction of the sickle mutation amplified in vivo during erythroid differentiation. bioRxiv, 432716.

19. Forget, B.G. (1998). Molecular basis of hereditary persistence of fetal hemoglobin. Ann. NY Acad. Sci *850*, 38–44.

20. Traxler, E.A., Yao, Y., Wang, Y.-D., Woodard, K.J., Kurita, R., Nakamura, Y., Hughes, J.R., Hardison, R.C., Blobel, G.A., Li, C., and Weiss, M.J. (2016). A genome-editing strategy to treat β-hemoglobinopathies that recapitulates a mutation associated with a benign genetic condition. Nat. Med. *22*, 987–990.

21. Li, C., Psatha, N., Sova, P., Gil, S., Wang, H., Kim, J., Kulkarni, C., Valensisi, C., Hawkins, R.D., Stamatoyannopoulos, G., and Lieber, A. (2018). Reactivation of γ-globin in adult β-YAC mice after ex vivo and in vivo hematopoietic stem cell genome editing. Blood *131*, 2915–2928.

22. Lux, C.T., Pattabhi, S., Berger, M., Nourigat, C., Flowers, D.A., Negre, O., Humbert, O., Yang, J.G., Lee, C., Jacoby, K., et al. (2018). TALEN-mediated gene editing of *HBG* in human hematopoietic stem cells leads to therapeutic fetal hemoglobin induction. Mol. Ther. Methods Clin. Dev. *12*, 175–183.

23. Weber, L., Frati, G., Felix, T., Hardouin, G., Casini, A., Wollenschlaeger, C., Meneghini, V., Masson, C., De Cian, A., Chalumeau, A., et al. (2020). Editing a γ-globin repressor binding site restores fetal hemoglobin synthesis and corrects the sickle cell disease phenotype. Sci. Adv. *6*, eaay9392.

24. Antoniani, C., Meneghini, V., Lattanzi, A., Felix, T., Romano, O., Magrin, E., Weber, L., Pavani, G., El Hoss, S., Kurita, R., et al. (2018). Induction of fetal hemoglobin synthesis by CRISPR/Cas9-mediated editing of the human β-globin locus. Blood *131*, 1960–1973.

25. Brendel, C., Guda, S., Renella, R., Bauer, D.E., Canver, M.C., Kim, Y.J., Heeney, M.M., Klatt, D., Fogel, J., Milsom, M.D., et al. (2016). Lineage-specific BCL11A knockdown circumvents toxicities and reverses sickle phenotype. J. Clin. Invest. *126*, 3868–3878.

26. Canver, M.C., Smith, E.C., Sher, F., Pinello, L., Sanjana, N.E., Shalem, O., Chen, D.D., Schupp, P.G., Vinjamur, D.S., Garcia, S.P., et al. (2015). *BCL11A* enhancer dissection by Cas9-mediated in situ saturating mutagenesis. Nature *527*, 192–197.

27. Chang, K.-H., Smith, S.E., Sullivan, T., Chen, K., Zhou, Q., West, J.A., Liu, M., Liu, Y., Vieira, B.F., Sun, C., et al. (2017). Long-term engraftment and fetal globin induction upon *BCL11A* gene editing in bone-marrow-derived $CD34^+$ hematopoietic stem and progenitor cells. Mol. Ther. Methods Clin. Dev. *4*, 137–148.

28. Frangoul, H., Altshuler, D., Cappellini, M.D., Chen, Y.S., Domm, J., Eustace, B.K., Foell, J., de la Fuente, J., Grupp, S., Handgretinger, R., et al. (2021). CRISPR-Cas9 gene editing for sickle cell disease and β-thalassemia. N. Engl. J. Med. *384*, 252–260.

29. Liang, P., Xu, Y., Zhang, X., Ding, C., Huang, R., Zhang, Z., Lv, J., Xie, X., Chen, Y., Li, Y., et al. (2015). CRISPR/Cas9-mediated gene editing in human tripronuclear zygotes. Protein Cell *6*, 363–372.

30. Cradick, T.J., Fine, E.J., Antico, C.J., and Bao, G. (2013). CRISPR/Cas9 systems targeting β-globin and CCR5 genes have substantial off-target activity. Nucleic Acids Res. *41*, 9584–9592.

31. Kurita, R., Suda, N., Sudo, K., Miharada, K., Hiroyama, T., Miyoshi, H., Tani, K., and Nakamura, Y. (2013). Establishment of immortalized human erythroid progenitor cell lines able to produce enucleated red blood cells. PLoS ONE *8*, e59890.

32. Brinkman, E.K., Chen, T., Amendola, M., and van Steensel, B. (2014). Easy quantitative assessment of genome editing by sequence trace decomposition. Nucleic Acids Res. *42*, e168.

33. Luo, Y., Zhu, D., Zhang, Z., Chen, Y., and Sun, X. (2015). Integrative analysis of CRISPR/Cas9 target sites in the human HBB gene. Biomed. Res. Int. *2015*, 514709.

34. Cradick, T.J., Qiu, P., Lee, C.M., Fine, E.J., and Bao, G. (2014). COSMID: A web-based tool for identifying and validating CRISPR/Cas off-target sites. Mol. Ther. Nucleic Acids *3*, e214.

35. Dang, Y., Jia, G., Choi, J., Ma, H., Anaya, E., Ye, C., Shankar, P., and Wu, H. (2015). Optimizing sgRNA structure to improve CRISPR-Cas9 knockout efficiency. Genome Biol. *16*, 280.

36. Pavani, G., Fabiano, A., Laurent, M., Amor, F., Cantelli, E., Chalumeau, A., Maule, G., Tachtsidi, A., Concordet, J.P., Cereseto, A., et al. (2021). Correction of β-thalassemia by CRISPR/Cas9 editing of the α-globin locus in human hematopoietic stem cells. Blood Adv. *5*, 1137–1153.

37. Roselli, E.A., Mezzadra, R., Frittoli, M.C., Maruggi, G., Biral, E., Mavilio, F., Mastropietro, F., Amato, A., Tonon, G., Refaldi, C., et al. (2010). Correction of β-thalassemia major by gene transfer in haematopoietic progenitors of pediatric patients. EMBO Mol. Med. *2*, 315–328.

38. Esrick, E.B., Lehmann, L.E., Biffi, A., Achebe, M., Brendel, C., Ciuculescu, M.F., Daley, H., MacKinnon, B., Morris, E., Federico, A., et al. (2021). Post-transcriptional genetic silencing of *BCL11A* to treat sickle cell disease. N. Engl. J. Med. *384*, 205–215.

39. Ahle, S. (2020). Gene editing therapy shows early benefit for patients with SCD and beta thalassemia, https://www.ashclinicalnews.org/news/latest-and-greatest/crispr-shows-early-benefit-patients-sickle-cell-disease-beta-thalassemia/.

40. Smith, A.R., Schiller, G.J., Vercellotti, G.M., et al. (2019). Preliminary results of a phase 1/2 clinical study of zinc finger nuclease-mediated editing of BCL11A in autologous hematopoietic stem cells for transfusion-dependent beta thalassemia. Blood *134* (*Suppl 1*), 3544.

41. Sankaran, V.G., Menne, T.F., Xu, J., Akie, T.E., Lettre, G., Van Handel, B., Mikkola, H.K., Hirschhorn, J.N., Cantor, A.B., and Orkin, S.H. (2008). Human fetal hemoglobin expression is regulated by the developmental stage-specific repressor *BCL11A*. Science *322*, 1839–1842.

42. Yin, J., Xie, X., Ye, Y., Wang, L., and Che, F. (2019). BCL11A: A potential diagnostic biomarker and therapeutic target in human diseases. Biosci. Rep. *39*, BSR20190604.

43. Lattanzi, A., Meneghini, V., Pavani, G., Amor, F., Ramadier, S., Felix, T., Antoniani, C., Masson, C., Alibeu, O., Lee, C., et al. (2019). Optimization of CRISPR/Cas9 delivery to human hematopoietic stem and progenitor cells for therapeutic genomic rearrangements. Mol. Ther. *27*, 137–150.

44. Giarratana, M.-C., Kobari, L., Lapillonne, H., Chalmers, D., Kiger, L., Cynober, T., Marden, M.C., Wajcman, H., and Douay, L. (2005). Ex vivo generation of fully mature human red blood cells from hematopoietic stem cells. Nat. Biotechnol. *23*, 69–74.

45. Galanello, R., and Origa, R. (2010). Beta-thalassemia. Orphanet J. Rare Dis. *5*, 11.

46. Needs, T., Gonzalez-Mosquera, L.F., and Lynch, D.T. (2021). Beta thalassemia. In StatPearls [Internet] (StatPearls Publishing), https://www.ncbi.nlm.nih.gov/books/NBK531481/.

47. Thompson, A.A., Walters, M.C., Kwiatkowski, J., Rasko, J.E.J., Ribeil, J.A., Hongeng, S., Magrin, E., Schiller, G.J., Payen, E., Semeraro, M., et al. (2018). Gene therapy in patients with transfusion-dependent β-thalassemia. N. Engl. J. Med. *378*, 1479–1493.

48. Seminog, O.O., Ogunlaja, O.I., Yeates, D., and Goldacre, M.J. (2016). Risk of individual malignant neoplasms in patients with sickle cell disease: English national record linkage study. J. R. Soc. Med. *109*, 303–309.

49. Brunson, A., Keegan, T.H.M., Bang, H., Mahajan, A., Paulukonis, S., and Wun, T. (2017). Increased risk of leukemia among sickle cell disease patients in California. Blood *130*, 1597–1599.

50. Breda, L., Ghiaccio, V., Tanaka, N., Jarocha, D., Ikawa, Y., Abdulmalik, O., Dong, A., Casu, C., Raabe, T.D., Shan, X., et al. (2021). Lentiviral vector ALS20 yields high hemoglobin levels with low genomic integrations for treatment of beta-globinopathies. Mol. Ther. *29*, 1625–1638.

51. Akinsheye, I., Alsultan, A., Solovieff, N., Ngo, D., Baldwin, C.T., Sebastiani, P., Chui, D.H., and Steinberg, M.H. (2011). Fetal hemoglobin in sickle cell anemia. Blood *118*, 19–27.

52. Steinberg, M.H., Chui, D.H.K., Dover, G.J., Sebastiani, P., and Alsultan, A. (2014). Fetal hemoglobin in sickle cell anemia: A glass half full? Blood *123*, 481–485.

53. Yudovich, D., Bäckström, A., Schmiderer, L., Žemaitis, K., Subramaniam, A., and Larsson, J. (2020). Combined lentiviral- and RNA-mediated CRISPR/Cas9 delivery for efficient and traceable gene editing in human hematopoietic stem and progenitor cells. Sci. Rep. *10*, 22393.

54. Ting, P.Y., Parker, A.E., Lee, J.S., Trussell, C., Sharif, O., Luna, F., Federe, G., Barnes, S.W., Walker, J.R., Vance, J., et al. (2018). Guide Swap enables genome-scale pooled CRISPR-Cas9 screening in human primary cells. Nat. Methods *15*, 941–946.

55. Martyn, G.E., Wienert, B., Yang, L., Shah, M., Norton, L.J., Burdach, J., Kurita, R., Nakamura, Y., Pearson, R.C.M., Funnell, A.P.W., et al. (2018). Natural regulatory mutations elevate the fetal globin gene via disruption of BCL11A or ZBTB7A binding. Nat. Genet. *50*, 498–503.

56. Liu, N., Xu, S., Yao, Q., Zhu, Q., Kai, Y., Hsu, J.Y., Sakon, P., Pinello, L., Yuan, G.C., Bauer, D.E., and Orkin, S.H. (2021). Transcription factor competition at the γ-globin promoters controls hemoglobin switching. Nat. Genet. *53*, 511–520.

57. Chaudhari, H.G., Penterman, J., Whitton, H.J., Spencer, S.J., Flanagan, N., Lei Zhang, M.C., Huang, E., Khedkar, A.S., Toomey, J.M., Shearer, C.A., et al. (2020). Evaluation of homology-independent CRISPR-Cas9 off-target assessment methods. CRISPR J. *3*, 440–453.

58. Shapiro, J., Iancu, O., Jacobi, A.M., McNeill, M.S., Turk, R., Rettig, G.R., Amit, I., Tovin-Recht, A., Yakhini, Z., Behlke, M.A., and Hendel, A. (2020). Increasing CRISPR efficiency and measuring its specificity in HSPCs using a clinically relevant system. Mol. Ther. Methods Clin. Dev. *17*, 1097–1107.

59. Tsai, S.Q., and Joung, J.K. (2016). Defining and improving the genome-wide specificities of CRISPR-Cas9 nucleases. Nat. Rev. Genet. *17*, 300–312.

60. Wu, Y., Zeng, J., Roscoe, B.P., Liu, P., Yao, Q., Lazzarotto, C.R., Clement, K., Cole, M.A., Luk, K., Baricordi, C., et al. (2019). Highly efficient therapeutic gene editing of human hematopoietic stem cells. Nat. Med. *25*, 776–783.

61. Gaziev, J., and Lucarelli, G. (2003). Stem cell transplantation for hemoglobinopathies. Curr. Opin. Pediatr. *15*, 24–31.

62. Cromer, M.K., Vaidyanathan, S., Ryan, D.E., Curry, B., Lucas, A.B., Camarena, J., Kaushik, M., Hay, S.R., Martin, R.M., Steinfeld, I., et al. (2018). Global transcriptional response to CRISPR/Cas9-AAV6-based genome editing in $CD34^{+}$ hematopoietic stem and progenitor cells. Mol. Ther. *26*, 2431–2442.

63. Uchida, N., Drysdale, C.M., Nassehi, T., Gamer, J., Yapundich, M., DiNicola, J., Shibata, Y., Hinds, M., Gudmundsdottir, B., Haro-Mora, J.J., et al. (2021). Cas9 protein delivery non-integrating lentiviral vectors for gene correction in sickle cell disease. Mol. Ther. Methods Clin. Dev. *21*, 121–132.

64. Chang, H.H.Y., Pannunzio, N.R., Adachi, N., and Lieber, M.R. (2017). Non-homologous DNA end joining and alternative pathways to double-strand break repair. Nat. Rev. Mol. Cell Biol. *18*, 495–506.

65. Hustedt, N., and Durocher, D. (2016). The control of DNA repair by the cell cycle. Nat. Cell Biol. *19*, 1–9.

66. Nakamura, K., Saredi, G., Becker, J.R., Foster, B.M., Nguyen, N.V., Beyer, T.E., Cesa, L.C., Faull, P.A., Lukauskas, S., Frimurer, T., et al. (2019). H4K20me0 recognition by BRCA1-BARD1 directs homologous recombination to sister chromatids. Nat. Cell Biol. *21*, 311–318.

67. Vítor, A.C., Huertas, P., Legube, G., and de Almeida, S.F. (2020). Studying DNA double-strand break repair: An ever-growing toolbox. Front. Mol. Biosci. *7*, 24.

68. Magis, W., DeWitt, M.A., Wyman, S.K., Vu, J.T., Heo, S.-J., Shao, S.J., Hennig, F., Romero, Z.G., Campo-Fernandez, B., McNeill, M., et al. (2018). High-level correction of the sickle mutation amplified in vivo during erythroid differentiation. bioRxiv. https://doi.org/10.1101/432716.

69. Frangoul, H., Bobruff, Y., Cappellini, M.D., Corbacioglu, S., Fernandez, C.M., de la Fuente, J., Grupp, S.A., Handgretinger, R., Ho, T.W., Imren, S., et al. (2020). Safety and efficacy of CTX001 in patients with transfusion-dependent β-thalassemia and sickle cell disease: Early results from the Climb THAL-111 and Climb SCD-121 studies of autologous CRISPR-CAS9-Modified CD34+ hematopoietic stem and progenitor cells. Blood *136* (*Suppl 1*), 3–4.

70. Gaudelli, N.M., Lam, D.K., Rees, H.A., Solá-Esteves, N.M., Barrera, L.A., Born, D.A., Edwards, A., Gehrke, J.M., Lee, S.J., Liquori, A.J., et al. (2020). Directed evolution of adenine base editors with increased activity and therapeutic application. Nat. Biotechnol. *38*, 892–900.

71. Richter, M.F., Zhao, K.T., Eton, E., Lapinaite, A., Newby, G.A., Thuronyi, B.W., Wilson, C., Koblan, L.W., Zeng, J., Bauer, D.E., et al. (2020). Phage-assisted evolution of an adenine base editor with improved Cas domain compatibility and activity. Nat. Biotechnol. *38*, 883–891.

72. Rees, H.A., and Liu, D.R. (2018). Base editing: Precision chemistry on the genome and transcriptome of living cells. Nat. Rev. Genet. *19*, 770–788.

73. Nakamura, M., Gao, Y., Dominguez, A.A., and Qi, L.S. (2021). CRISPR technologies for precise epigenome editing. Nat. Cell Biol. *23*, 11–22.

74. Anzalone, A.V., Randolph, P.B., Davis, J.R., Sousa, A.A., Koblan, L.W., Levy, J.M., Chen, P.J., Wilson, C., Newby, G.A., Raguram, A., and Liu, D.R. (2019). Search-and-replace genome editing without double-strand breaks or donor DNA. Nature *576*, 149–157.

75. Hardison, R., Slightom, J.L., Gumucio, D.L., Goodman, M., Stojanovic, N., and Miller, W. (1997). Locus control regions of mammalian beta-globin gene clusters: Combining phylogenetic analyses and experimental results to gain functional insights. Gene *205*, 73–94.

76. Lattanzi, A., Duguez, S., Moiani, A., Izmiryan, A., Barbon, E., Martin, S., Mamchaoui, K., Mouly, V., Bernardi, F., Mavilio, F., and Bovolenta, M. (2017). Correction of the exon 2 duplication in DMD myoblasts by a single CRISPR/Cas9 system. Mol. Ther. Nucleic Acids *7*, 11–19.

77. Zonari, E., Desantis, G., Petrillo, C., Boccalatte, F.E., Lidonnici, M.R., Kajaste-Rudnitski, A., Aiuti, A., Ferrari, G., Naldini, L., and Gentner, B. (2017). Efficient ex vivo engineering and expansion of highly purified human hematopoietic stem and progenitor cell populations for gene therapy. Stem Cell Reports *8*, 977–990.

78. Delville, M., Soheili, T., Bellier, F., Durand, A., Denis, A., Lagresle-Peyrou, C., Cavazzana, M., Andre-Schmutz, I., and Six, E. (2018). A nontoxic transduction enhancer enables highly efficient lentiviral transduction of primary murine T cells and hematopoietic stem cells. Mol. Ther. Methods Clin. Dev. *10*, 341–347.

79. Bon, P., Maucort, G., Wattellier, B., and Monneret, S. (2009). Quadriwave lateral shearing interferometry for quantitative phase microscopy of living cells. Opt. Express *17*, 13080–13094.

80. Aknoun, S., Savatier, J., Bon, P., Galland, F., Abdeladim, L., Wattellier, B., and Monneret, S. (2015). Living cell dry mass measurement using quantitative phase imaging with quadriwave lateral shearing interferometry: An accuracy and sensitivity discussion. J. Biomed. Opt. *20*, 126009.

YMTHE, Volume *30*

Supplemental Information

Combination of lentiviral and genome editing technologies for the treatment of sickle cell disease

Sophie Ramadier, Anne Chalumeau, Tristan Felix, Nadia Othman, Sherazade Aknoun, Antonio Casini, Giulia Maule, Cecile Masson, Anne De Cian, Giacomo Frati, Megane Brusson, Jean-Paul Concordet, Marina Cavazzana, Anna Cereseto, Wassim El Nemer, Mario Amendola, Benoit Wattellier, Vasco Meneghini, and Annarita Miccio

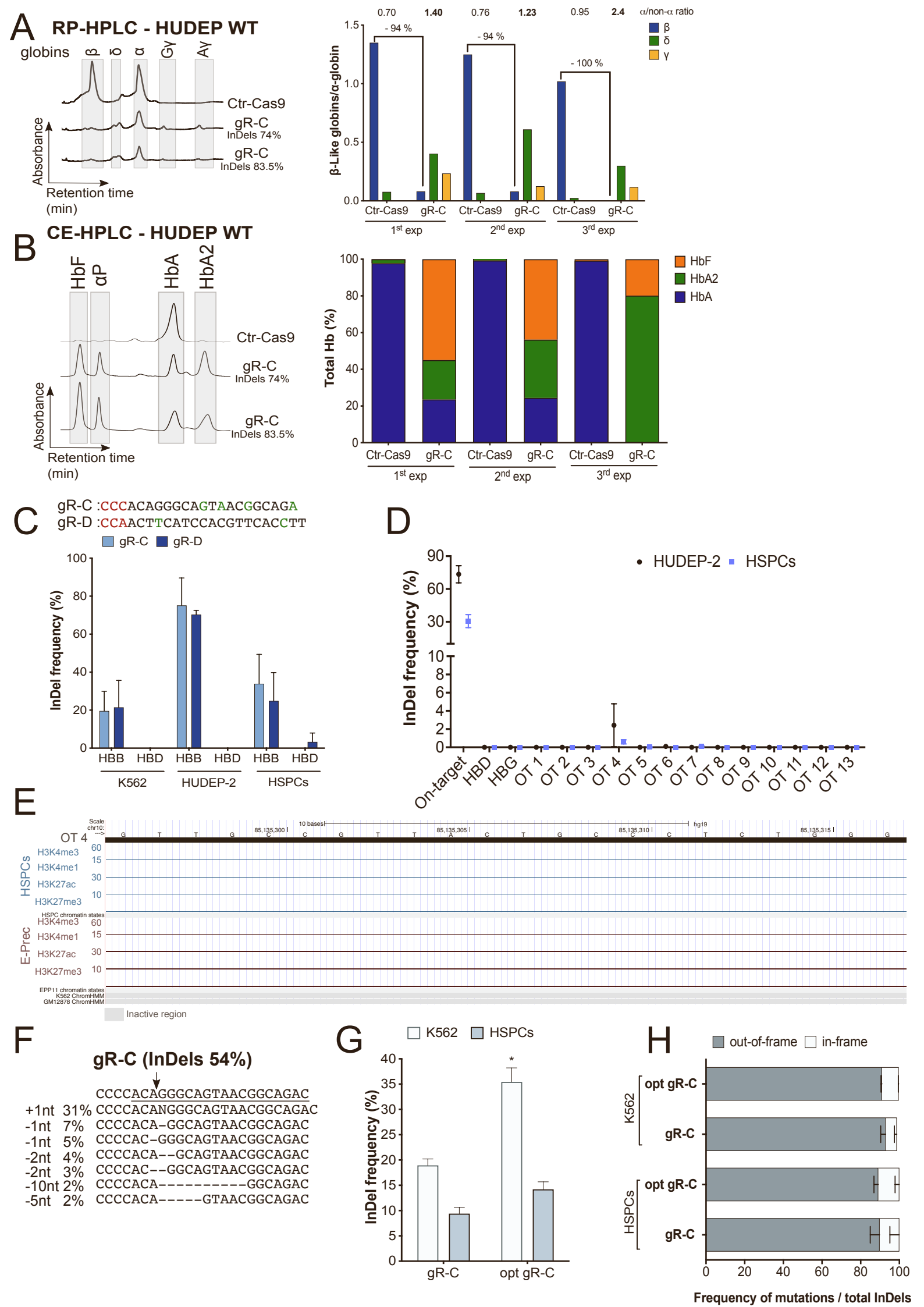
A
RP-HPLC - HUDEP WT
globins
β
δ
α
Gγ
Aγ
Ctr-Cas9
gR-C
InDels 74%
gR-C
InDels 83.5%
Absorbance
Retention time
(min)
0.70
1.40
0.76
1.23
0.95
2.4
α/non-α ratio
β
δ
γ
- 94 %
- 94 %
- 100 %
β-Like globins/α-globin
Ctr-Cas9
gR-C
1st exp
2nd exp
3rd exp
B
CE-HPLC - HUDEP WT
HbF
αP
HbA
HbA2
Ctr-Cas9
gR-C
InDels 74%
gR-C
InDels 83.5%
Absorbance
Retention time
(min)
HbF
HbA2
HbA
Total Hb (%)
C
gR-C :CCCACAGGGCAGTAACGGCAGA
gR-D :CCAACTTCATCCACGTTCACCTT
gR-C
gR-D
InDel frequency (%)
HBB
HBD
K562
HUDEP-2
HSPCs
D
HUDEP-2
HSPCs
InDel frequency (%)
On-target
HBD
HBG
OT 1
OT 2
OT 3
OT 4
OT 5
OT 6
OT 7
OT 8
OT 9
OT 10
OT 11
OT 12
OT 13
E
OT 4
HSPCs
H3K4me3
H3K4me1
H3K27ac
H3K27me3
HSPC chromatin states
E-Prec
EPP11 chromatin states
K562 ChromHMM
GM12878 ChromHMM
Inactive region
F
gR-C (InDels 54%)
CCCCACAGGGCAGTAACGGCAGAC
+1nt 31% CCCCACANGGGCAGTAACGGCAGAC
-1nt 7% CCCCACA-GGCAGTAACGGCAGAC
-1nt 5% CCCCAC-GGGCAGTAACGGCAGAC
-2nt 4% CCCCACA--GCAGTAACGGCAGAC
-2nt 3% CCCCAC--GGCAGTAACGGCAGAC
-10nt 2% CCCCACA----------GGCAGAC
-5nt 2% CCCCACA-----GTAACGGCAGAC
G
K562
HSPCs
InDel frequency (%)
gR-C
opt gR-C
H
out-of-frame
in-frame
K562
opt gR-C
gR-C
HSPCs
opt gR-C
gR-C
Frequency of mutations / total InDels

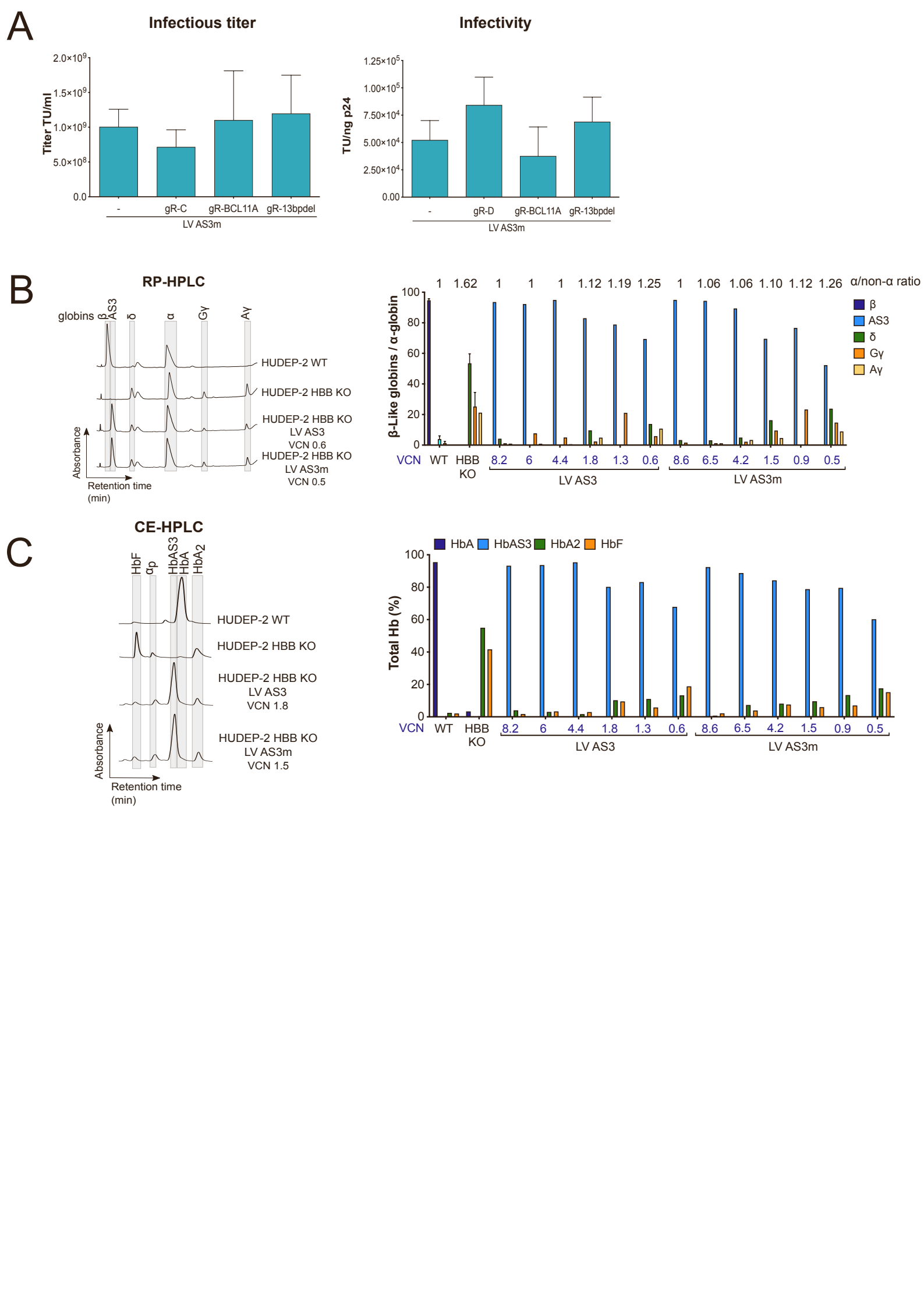
A
Infectious titer
Titer TU/ml
2.0×10^9
1.5×10^9
1.0×10^9
5.0×10^8
0.0
-
gR-C
gR-BCL11A
gR-13bpdel
LV AS3m
Infectivity
TU/ng p24
1.25×10^5
1.00×10^5
7.50×10^4
5.00×10^4
2.50×10^4
0.00
-
gR-D
gR-BCL11A
gR-13bpdel
LV AS3m
B
RP-HPLC
globins
β AS3
δ
α
Gγ
Aγ
HUDEP-2 WT
HUDEP-2 HBB KO
HUDEP-2 HBB KO LV AS3 VCN 0.6
HUDEP-2 HBB KO LV AS3m VCN 0.5
Absorbance
Retention time (min)
β-Like globins / α-globin
α/non-α ratio
1 1.62 1 1 1 1.12 1.19 1.25 1 1.06 1.06 1.10 1.12 1.26
β
AS3
δ
Gγ
Aγ
VCN WT HBB KO 8.2 6 4.4 1.8 1.3 0.6 8.6 6.5 4.2 1.5 0.9 0.5
LV AS3
LV AS3m
C
CE-HPLC
HbF
αp
HbAS3
HbA
HbA2
HUDEP-2 WT
HUDEP-2 HBB KO
HUDEP-2 HBB KO LV AS3 VCN 1.8
HUDEP-2 HBB KO LV AS3m VCN 1.5
Absorbance
Retention time (min)
Total Hb (%)
HbA HbAS3 HbA2 HbF
VCN WT HBB KO 8.2 6 4.4 1.8 1.3 0.6 8.6 6.5 4.2 1.5 0.9 0.5
LV AS3
LV AS3m

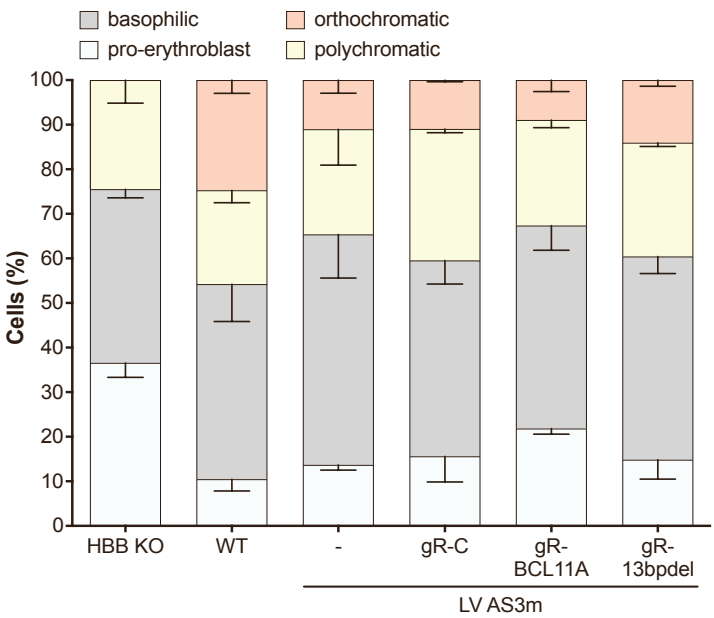
basophilic
orthochromatic
pro-erythroblast
polychromatic
Cells (%)
100
90
80
70
60
50
40
30
20
10
0
HBB KO
WT
-
gR-C
gR-BCL11A
gR-13bpdel
LV AS3m

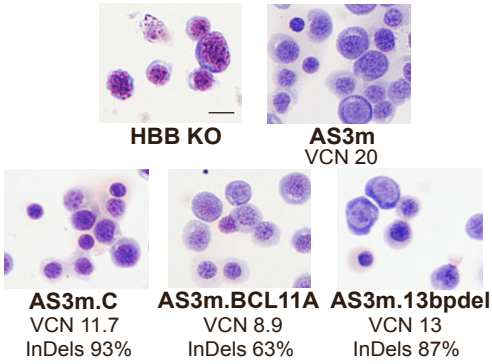
HBB KO
AS3m
VCN 20
AS3m.C
VCN 11.7
InDels 93%
AS3m.BCL11A
VCN 8.9
InDels 63%
AS3m.13bpdel
VCN 13
InDels 87%

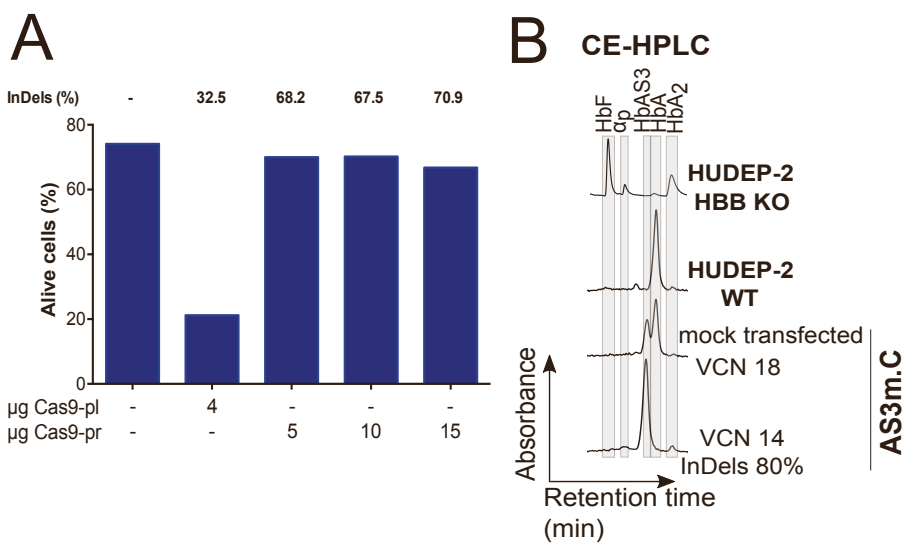
A
InDels (%) - 32.5 68.2 67.5 70.9
Alive cells (%)
0
20
40
60
80
µg Cas9-pl - 4 - - -
µg Cas9-pr - - 5 10 15
B
CE-HPLC
HbF
αp
HbAS3
HbA
HbA2
HUDEP-2
HBB KO
HUDEP-2
WT
mock transfected
VCN 18
VCN 14
InDels 80%
Absorbance
Retention time
(min)
AS3m.C
HbA (mock transfected)
HbAS3 (mock transfected)
HbAS3 (Cas9 transfected)
HbA (Cas9 transfected)
% Hb/HbS+HbAS3
R2= 0.95
R2= 0.88
R2= 0.88
R2= 0.95
VCN

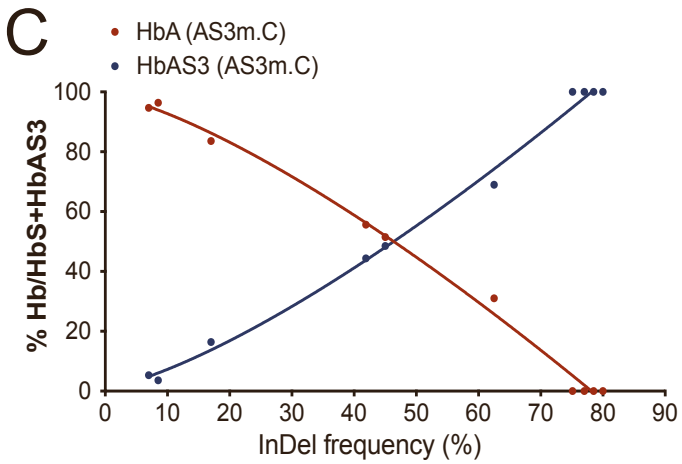
C
HbA (AS3m.C)
HbAS3 (AS3m.C)
% Hb/HbS+HbAS3
InDel frequency (%)

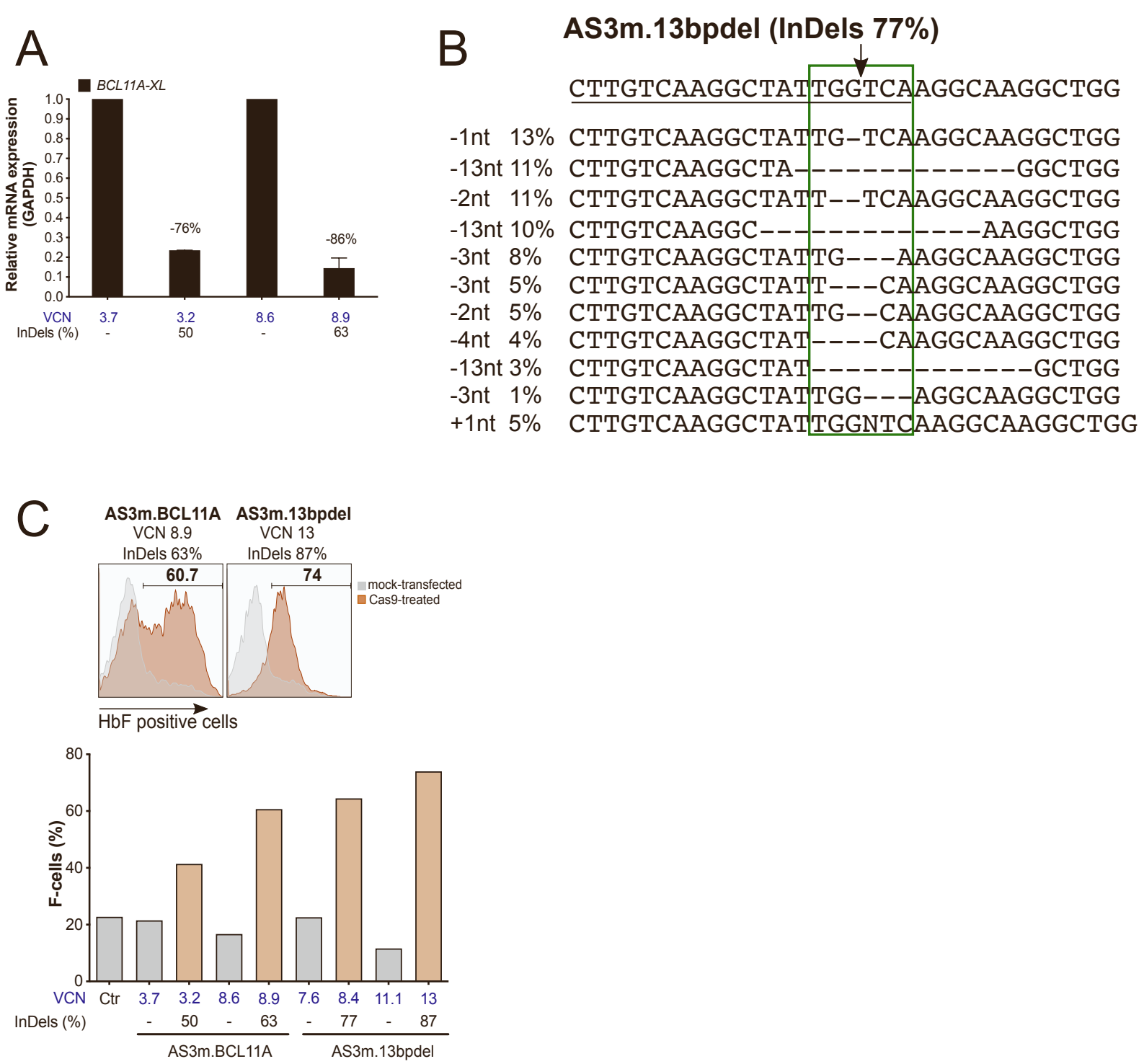
A
BCL11A-XL
Relative mRNA expression (GAPDH)
1.0
0.9
0.8
0.7
0.6
0.5
0.4
0.3
0.2
0.1
0.0
-76%
-86%
VCN 3.7 3.2 8.6 8.9
InDels (%) - 50 - 63
B
AS3m.13bpdel (InDels 77%)
CTTGTCAAGGCTATTGGTCAAGGCAAGGCTGG
-1nt 13% CTTGTCAAGGCTATTG-TCAAGGCAAGGCTGG
-13nt 11% CTTGTCAAGGCTA----------GGCTGG
-2nt 11% CTTGTCAAGGCTATT--TCAAGGCAAGGCTGG
-13nt 10% CTTGTCAAGGC----------AAGGCTGG
-3nt 8% CTTGTCAAGGCTATTG---AAGGCAAGGCTGG
-3nt 5% CTTGTCAAGGCTATT---CAAGGCAAGGCTGG
-2nt 5% CTTGTCAAGGCTATTG--CAAGGCAAGGCTGG
-4nt 4% CTTGTCAAGGCTAT----CAAGGCAAGGCTGG
-13nt 3% CTTGTCAAGGCTAT----------GCTGG
-3nt 1% CTTGTCAAGGCTATTGG---AGGCAAGGCTGG
+1nt 5% CTTGTCAAGGCTATTGGNTCAAGGCAAGGCTGG

C
AS3m.BCL11A
VCN 8.9
InDels 63%
AS3m.13bpdel
VCN 13
InDels 87%
60.7
74
mock-transfected
Cas9-treated
HbF positive cells
F-cells (%)
80
60
40
20
0
VCN Ctr 3.7 3.2 8.6 8.9 7.6 8.4 11.1 13
InDels (%) - 50 - 63 - 77 - 87
AS3m.BCL11A
AS3m.13bpdel

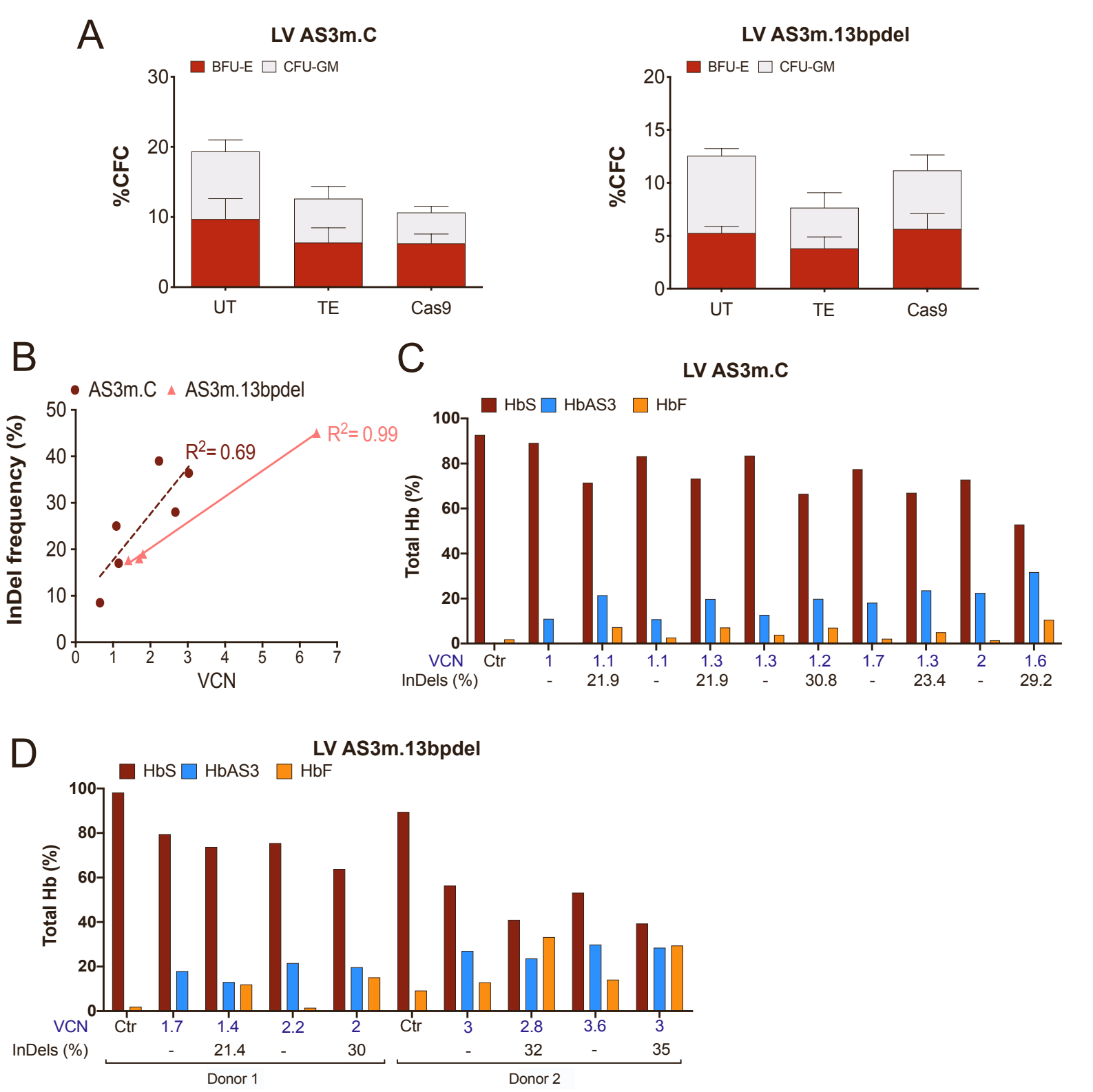
A
LV AS3m.C
BFU-E
CFU-GM
%CFC
30
20
10
0
UT
TE
Cas9
LV AS3m.13bpdel
BFU-E
CFU-GM
%CFC
20
15
10
5
0
UT
TE
Cas9
B
AS3m.C
AS3m.13bpdel
InDel frequency (%)
50
40
30
20
10
0
R2= 0.69
R2= 0.99
0
1
2
3
4
5
6
7
VCN
C
LV AS3m.C
HbS
HbAS3
HbF
Total Hb (%)
100
80
60
40
20
0
VCN
Ctr
1
1.1
1.1
1.3
1.3
1.2
1.7
1.3
2
1.6
InDels (%)
-
21.9
-
21.9
-
30.8
-
23.4
-
29.2
D
LV AS3m.13bpdel
HbS
HbAS3
HbF
Total Hb (%)
100
80
60
40
20
0
VCN
Ctr
1.7
1.4
2.2
2
Ctr
3
2.8
3.6
3
InDels (%)
-
21.4
-
30
-
32
-
35
Donor 1
Donor 2

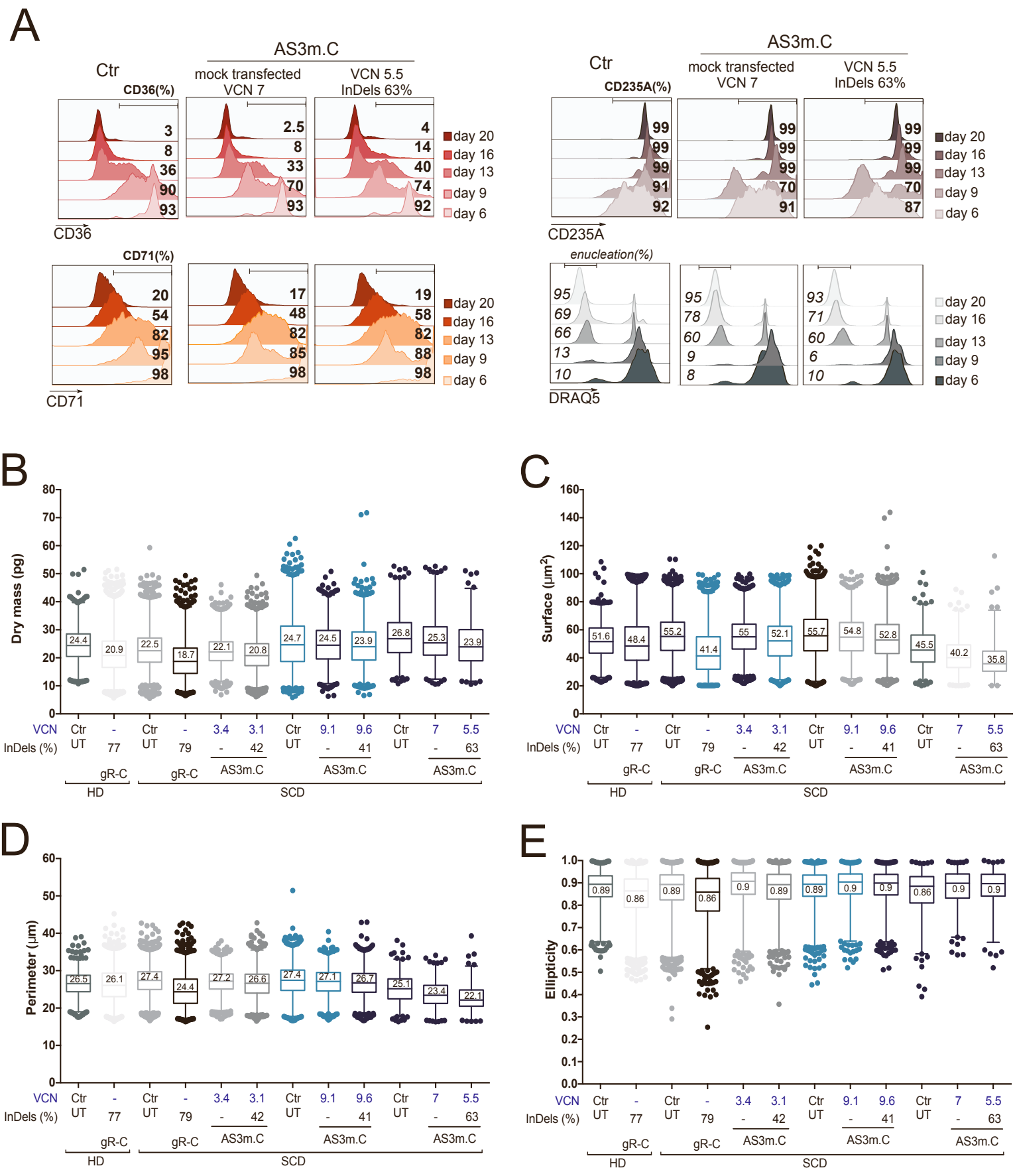
A
AS3m.C
Ctr
mock transfected VCN 7
VCN 5.5 InDels 63%
CD36(%)
3
8
36
90
93
2.5
8
33
70
93
4
14
40
74
92
day 20
day 16
day 13
day 9
day 6
CD36
CD71(%)
20
54
82
95
98
17
48
82
85
98
19
58
82
88
98
CD71
CD235A(%)
99
99
99
91
92
99
99
99
70
91
99
99
99
70
87
CD235A
enucleation(%)
95
69
66
13
10
95
78
60
9
8
93
71
60
6
10
DRAQ5
B
Dry mass (pg)
C
Surface (µm²)
D
Perimeter (µm)
E
Ellipticity
VCN
InDels (%)
Ctr UT
77
79
3.4
3.1
42
9.1
9.6
41
7
5.5
63
gR-C
AS3m.C
HD
SCD

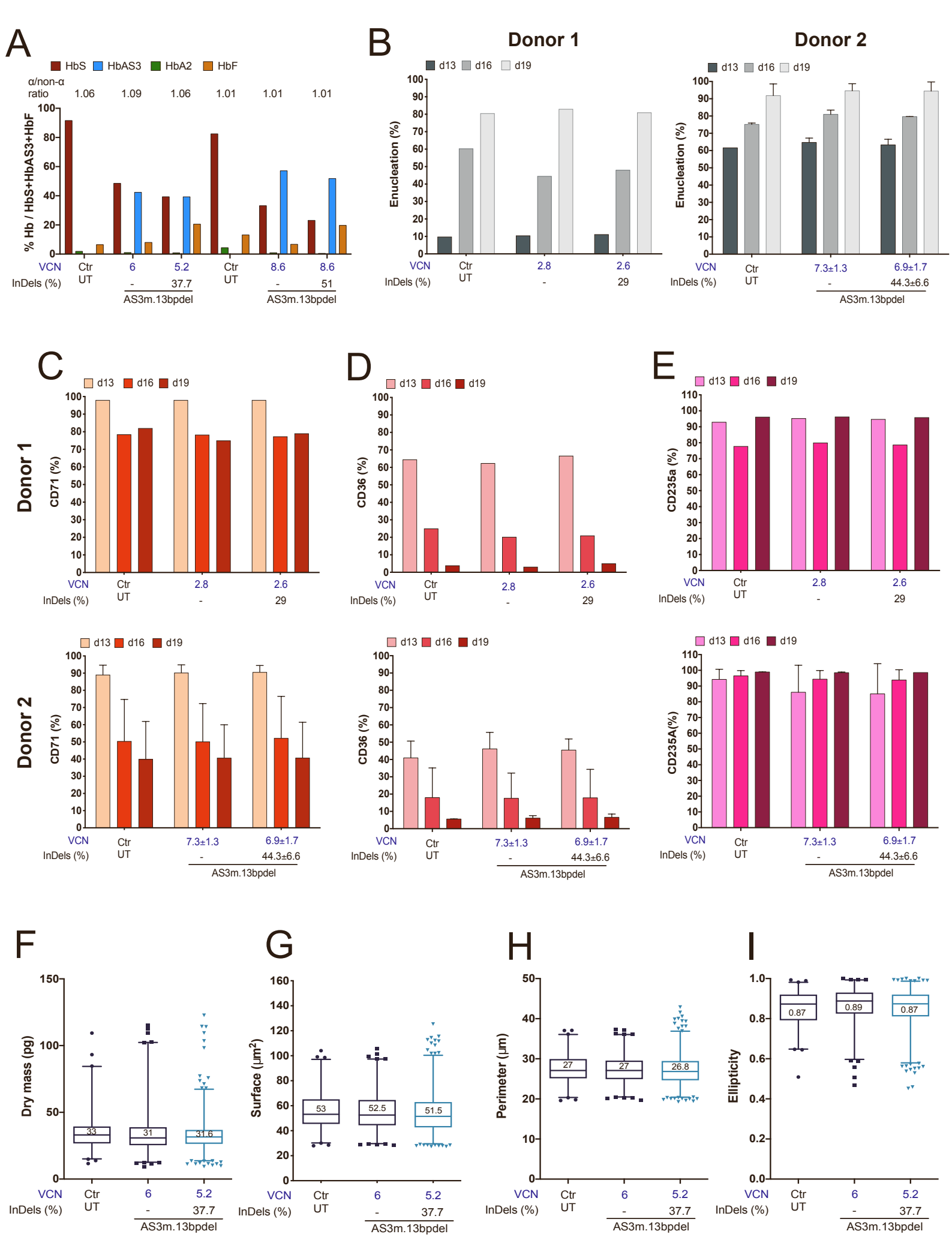
A
HbS
HbAS3
HbA2
HbF
α/non-α ratio
1.06
1.09
1.06
1.01
1.01
1.01
% Hb / HbS+HbAS3+HbF
VCN
Ctr UT
6
5.2
Ctr UT
8.6
8.6
InDels (%)
-
37.7
-
51
AS3m.13bpdel
AS3m.13bpdel
B
Donor 1
Donor 2
d13
d16
d19
Enucleation (%)
VCN
Ctr UT
2.8
2.6
InDels (%)
-
29
7.3±1.3
6.9±1.7
-
44.3±6.6
AS3m.13bpdel
C
D
E
Donor 1
Donor 2
CD71 (%)
CD36 (%)
CD235a (%)
CD235A(%)
VCN
Ctr UT
2.8
2.6
InDels (%)
-
29
7.3±1.3
6.9±1.7
-
44.3±6.6
AS3m.13bpdel
F
G
H
I
Dry mass (pg)
Surface (µm²)
Perimeter (µm)
Ellipticity
33
31
31.6
53
52.5
51.5
27
27
26.8
0.87
0.89
0.87
VCN
Ctr UT
6
5.2
InDels (%)
-
37.7
AS3m.13bpdel

Supplementary Figure Legends

Supplementary figure 1: Efficiency and safety analysis of sgRNAs knocking down the *HBB* gene.

(A) RP-HPLC analysis of globin chains in differentiated HUDEP-2 cells transfected with Cas9-GFP plasmid only (Ctr-Cas9) or with both Cas9-GFP and gR-C plasmids (gR-C). Representative chromatograms are reported in the left panel. Quantification is reported in the right panel. β-like globin chains were normalized to the α-globin chains. The percentage of β-globin decrease is reported above the histogram bars. α-/non-α ratios are reported on top of each sample (n=3; genome editing efficiency of 80.1±3.0 (mean±SEM)). **(B)** CE-HPLC quantification of Hb tetramers in HUDEP-2 cells transfected with Cas9-GFP plasmid only (Ctr-Cas9) or with both Cas9-GFP and gR-C plasmids (gR-C). Representative chromatograms are reported in the left panel. Quantification is reported in the right panel. We calculated the percentage of each Hb type over the total Hb tetramers. αP=α-precipitates **(C)** On- and off-target activity evaluated by TIDE in *HBB* and *HBD* in K562 (n=6 for gR-C and n=5 for gR-D in *HBB;* n=6 for gR-C and gR-D in *HBD*), HUDEP-2 (n=4 for gR-C and gR-D in *HBB* and *HBD*) and cord blood (CB) HSPCs edited with gR-C (n=3) or D (n=2) . Sequences of gR-C and D are reported above the graph; mismatches between the sgRNA target sequence and the potential off-target in *HBD* are indicated in green. PAM is indicated in red. Data are expressed as mean±SEM. **(D)** Editing efficiency of the *HBB* (On-target), *HBD*, *HBG* genes and the top 13 off-target sites (OT) identified by COSMID in HUDEP-2 (n=4 for *HBB* and *HBD*; n=3 for *HBG*, OT 1. OT 3, OT 4, OT 6, OT 8, OT 9, OT 11 and OT 12; n= 2 for OT 2, OT 5 , OT 7, OT 10 and OT 13) and CB HSPCs edited with gR-C (n=5), as measured by TIDE. Data are expressed as mean±SEM. Off-target editing was detected only for OT 4. Its closest genes are Neuregulin 3 (NRG3) (located 300 kb far from off-target 4), which is mainly expressed in CNS tissues, and AL356140.1 miRNA (located 68 kb far from the off-target site) with unknown functions and potentially involved in angiogenesis. **(E)** Analysis of the chromatin states at the OT 4 sequence in primary human HSPCs

and HSPC-derived erythroid precursors (E-Prec)[1], and in erythroid (K562) and granulo-monocytic (GM12878) cell lines (UCSC datasets). OT 4 maps to an inactive region in all the cell types. **(F)** Representative Sanger sequencing analysis of edited *HBB* alleles in G-CSF mPB HD HSPCs (54% of total InDels) using ICE Analysis[2]. The top line shows the unmodified *HBB* gene sequence. gR-C-targeted sequence is underlined. The arrow indicates the cleavage site. Dashes and "N" indicate deleted and inserted nucleotides, respectively. InDel type, length and frequency are indicated on the left. **(G)** Editing efficiency and **(H)** out-of-frame mutations evaluated by TIDE analysis after PCR amplification of the target region and Sanger sequencing in K562 (n=2; unpaired t test *$p<0.05$) and mobilized peripheral blood HD HSPCs edited with gR-C harboring the original (gR-C; n=3) or the optimized (opt gR-C; n=4) scaffold. Data are expressed as mean±SEM.

Supplementary figure 2: Bifunctional LVs expressing an *HBB* modified transgene.

(A) Histograms showing: (i) the infectious titer (left panel) of LV AS3m "-" (n=6) and LV AS3m containing gR-C (n=6), gR-BCL11A (n=5) and gR-13bpdel (n=5); (ii) infectivity (right panel) of LV AS3m "-" (n=4) and LV AS3m containing gR-C (n=6), gR-BCL11A (n=3) and gR-13bpdel (n=3). Titer and infectivity were evaluated in HCT116 cells. The infectivity was measured as a ratio between the infectious (TU/ml) and the physical titer (ng p24/ml). Data are expressed as mean±SEM. **(B)** RP-HPLC chromatograms (left panel) and quantification (right panel) of globin chains in LV AS3- and LV AS3m-treated cells. WT HUDEP-2 and HBB KO HUDEP-2 served as controls. β-like globin chains are normalized to α-globin chains. VCN are reported in blue below the graph. α/non-α ratios are reported above the histogram bars. **(C)** CE-HPLC chromatograms (left panel) and quantification (right panel) of Hb tetramers in LV AS3- and LV AS3m-treated cells. WT HUDEP-2 and HBB KO HUDEP-2 served as controls. We plotted the percentage of each Hb type over the total Hbs. VCN are reported in blue below the graph.

Supplementary figure 3: LV-treated-HUDEP-2 cells can differentiate into mature erythroblasts.

Quantification (left panel) and representative photomicrographs (right panel) of HUDEP-2 erythroid precursors obtained at day 9 of the erythroid differentiation and stained with May-Grünwald Giemsa. HBB KO, WT and mock-transfected HUDEP-2 cells served as controls. HUDEP-2 HBB KO cells display a higher percentage of immature pro-erythroblasts and absence of more mature orthochromatic cells compared to WT cells. Data are expressed as mean±SEM. Scale bar, 40 µm (upper left).

Supplementary figure 4: Superior efficiency of Cas9-GFP protein compared to Cas9-GFP plasmid in LV AS3m.C-transduced HUDEP-2 cells.

(A) A representative experiment showing the percentage of alive HUDEP-2 cells measured by flow cytometry 24 hours after transfection with either Cas9-GFP plasmid (4 µg) or Cas9-GFP protein (5-15 µg). InDel frequency is reported above the histograms. The proportion of alive cells was significantly lower in plasmid-transfected samples (37±6%) compared to untransfected cells (68±4%; $p<0.005$) or to samples transfected with 15 µg of Cas9-GFP protein (58±4%; $p<0.05$). No significative differences were observed between untransfected and Cas9-GFP protein-treated samples (n=3-4). **(B)** CE-HPLC chromatograms (left panel) and correlation between VCN and percentage of HbA or HbAS3 over the total adult tetramers (HbA+HbAS3) (right panel) in LV AS3m.C-transduced HUDEP-2 cells transfected with 15 µg of Cas9-GFP protein or mock-transfected. R^2 and line-of-best-fit equation are indicated. **(C)** Correlation between InDel frequency and percentage of HbA or HbAS3 over the total adult tetramers (HbA+HbAS3) in LV AS3m.C-transduced HUDEP-2 cells transfected with Cas9-GFP protein or mock-transfected. R^2 and line-of-best-fit equation are indicated.

Supplementary figure 5: Bifunctional LVs reactivate HbF expression.

(A) Relative expression of *BCL11A-XL* normalized to GAPDH, as measured by qRT-PCR in LV AS3m.BCL11A-transduced HUDEP-2 cells treated with Cas9-GFP plasmid or mock-transfected control ("-"). VCN are reported in blue and InDels in black below the graph. Data are expressed as mean ± SEM. **(B)** Representative Sanger sequencing analysis of edited *HBG* promoters in HUDEP-2 cells (77% of total InDels) using ICE Analysis[2]. The top line shows the unmodified *HBG1/2* promoter sequence. sgRNA 13bpdel-targeted sequence is underlined. The arrow indicates the cleavage site. The BCL11A binding site is highlighted with a green rectangle. Dashes and "N" indicate deleted and inserted nucleotides, respectively. InDel type, length and frequency are indicated on the left. **(C)** Representative flow cytometry plots (upper panel) and quantification (bottom panel) of HbF-expressing cells in untreated HUDEP-2 cells (Ctr), Cas9-treated and mock-transfected "-" HUDEP-2 cells transduced either with LV AS3m.BCL11A or LVAS3m.13bpdel. VCN are reported in blue and InDels in black below the graph.

Supplementary figure 6: Correlation between VCN and editing frequency in BFU-E transduced with bifunctional LVs

(A) Frequency of CFC in edited SCD HSPCs (Cas9). LV AS3m.C and LV AS3m.13bpdel-transduced SCD HSPCs transfected only with TE (TE) or untransfected (UT) were used as control. Data are expressed as mean±SEM (n=4-9; 2 mobilized SCD donors). **(B)** VCN and InDel frequency were determined in burst forming unit-erythroid (BFUE) derived from SCD HSPCs transduced either with LV AS3m.C or LV AS3m.13bpdel and transfected with Cas9-GFP protein. R^2 and line-of-best-fit equation are indicated. **(C)** CE-HPLC quantification of Hb tetramers in RBCs derived from untreated SCD HSPCs (Ctr) and LV AS3m.C-treated SCD HSPCs (1 donor) that were mock-transfected ("-") or transfected with Cas9-GFP protein. We plotted the percentage of each Hb type over the total Hb tetramers. VCN are reported in blue and InDels in black below the graph. **(D)** CE-HPLC quantification of Hb tetramers in RBCs obtained from untreated SCD HSPCs (Ctr) and LV AS3m.13bpdel-treated SCD HSPCs (2 donors) that were mock-transfected ("-") or transfected with

Cas9-GFP protein. We plotted the percentage of each Hb type over the total Hb tetramers. VCN are reported in blue and InDels in black below the graph.

Supplementary figure 7: Erythroid differentiation and RBC parameters in cells derived from LV AS3m.C-edited SCD HSPCs

(A) Representative flow cytometry analysis of the early (CD36 and CD71) and late (CD235A) erythroid markers at day 6, 9, 13, 16 and 20 of erythroid differentiation of untreated SCD cells (Ctr) and LV AS3m.C-treated SCD HSPCs that were either mock-transfected or transfected with Cas9-GFP protein. The enucleation rate was measured using DRAQ5 nuclear staining. **(B-E)** RBC parameters extracted using the BIO-Data software. RBCs were obtained after 19 days of differentiation from SCD HSPCs transduced with LV AS3m.C and either mock- or Cas9-transfected. As controls, we used untreated SCD RBCs (Ctr UT), and RBCs obtained from SCD/HD HSPCs transfected with RNPs containing gR-C (gR-C). For each population, data were normalized to the total number of RBCs and are reported as boxplots showing quartiles, median and outliers. Median value is indicated inside the boxplot. VCN are reported in blue and InDels in black below the graph. (**B**) Dry mass (pg). (**C**) Surface (μm^2). (**D**) Perimeter (µm). (**E**) Ellipticity.

Supplementary figure 8: Erythroid markers and RBC parameters were not impaired in cells derived from LV AS3m.13bpdel-edited SCD HSPCs.

(A) CE-HPLC quantification of Hb tetramers in untreated SCD cells (Ctr UT), and LV AS3m.13bpdel-treated SCD HSPCs that were either mock-transfected "-" or transfected with Cas9-GFP protein. We plotted the percentage of each Hb type over the total Hbs. VCN are reported in blue and InDels in black below the graph. The α-/non-α-globin ratios evaluated by RP-HPLC are reported on top of the histograms. **(B-E)** Flow cytometry analysis of the enucleation rate and of the early (CD71 and CD36) and late (CD235A) erythroid markers at day 13, 16 and 19 of erythroid differentiation of untreated SCD HSPCs (Ctr UT) and LV AS3m.13bpdel-treated SCD HSPCs that

were either mock-transfected or transfected with Cas9-GFP protein (n=3 biological replicates. 2 donors). VCN and InDels values are reported below the graph as mean±SEM. (**B**) Enucleation rate measured using DRAQ5 nuclear staining. (**C-E**) Proportion of $CD71^+$, $CD36^+$ and $CD235A^+$ cells during erythroid differentiation. **(F-I)** RBC parameters extracted using the BIO-Data software. RBCs were obtained after 19 days of differentiation from SCD HSPCs transduced with LV AS3m.13bpdel and either mock- or Cas9-transfected. As control, we used untreated SCD RBCs (Ctr UT). For each population, data were normalized to the total number of RBCs belonging and are reported as boxplots showing quartiles, median and outliers. Median value is indicated inside the boxplot. VCN are reported in blue and InDels in black below the graph. (**F**) Dry mass (pg). (**G**) Surface (μm^2). (**H**) Perimeter (µm). (**I**) Ellipticity.

Supplementary Methods

Plasmid construction

Plasmids expressing a Cas9-GFP fusion protein (pMJ920) and sgRNA (MLM3636) were purchased from Addgene (plasmids #42234 and #43860). The MA128 plasmid, containing the optimized sgRNA scaffold[3], was kindly provided by Dr. Amendola. The list of the sgRNA target sequences is provided in **Supplementary table 1.**

sgRNA name	Target sequence + PAM (5' to 3')	Strand	Hg19 genomic location
gR-A	gCTTGCCCCACAGGGCAGTAA**CGG**	-	chr11:5,226,968-5,226,987
gR-B	GTAACGGCAGACTTCTCCTC**AGG**	-	chr11:5,226,980-5,227,009

gR-C	gTCTGCCGTTACTGCCCTGT**GGG**	+	chr11:5,226,973-5,226,994
gR-D	gAAGGTGAACGTGGATGAAGT**TGG**	+	chr11:5,226,948-5,226,970

Supplementary Table 1: List of the sgRNAs targeting *HBB* exon 1. When the first nucleotide of the target sequence was different from a guanosine, we inserted a guanosine (indicated in lowercase) to allow U6-driven sgRNA expression. PAM sequences are highlighted in bold. For each sgRNA, we reported the hg19 genomic coordinates. gR-A sequence was retrieved from [4], gR-B sequence from [5], and gR-C and gR-D sequenced from [6].

HUDEP-2 and K562 cultures and differentiation

K562 were maintained in RPMI 1640 medium (Lonza) containing 2 mM glutamine and supplemented with 10% fetal bovine serum (FBS, BioWhittaker, Lonza), HEPES (20 mM, LifeTechnologies), sodium pyruvate (1 mM, LifeTechnologies) and penicillin/streptomycin (100U/ml each, LifeTechnologies).

HUDEP-2 cells[7] were cultured and differentiated for 8-9 days as previously described[8]. A standard May-Grumwald Giemsa staining was performed to evaluate the cell morphology during HUDEP-2 differentiation. Two fields per condition and a total of around 280 cells were counted. Erythroid differentiation was monitored during the culture by flow cytometry analysis.

HUDEP-2 thalassemic cells (HBB KO) were generated by transfecting HUDEP-2 WT cells with plasmids harboring the gR-D targeting *HBB* exon 1 and the Cas9-GFP. FACS-sorted GFP^+ cells were cloned by limiting dilution. After 14 days, single clones were isolated, expanded and screened by PCR and Sanger sequencing of the target sequence, followed by TIDE analysis. We selected a HUDEP-2 clone harboring bi-allelic frameshift mutations in the exon 1 of *HBB* gene and characterized by the absence of β-globin chain expression.

Lentiviral transduction of erythroid HUDEP-2 cell lines

Cells were transduced ($1x10^6$ cells/ml) for 24 h in the proliferation medium[8] supplemented with protamine sulfate (4 µg/ml, Sigma-Aldrich or APP Pharmaceuticals).

Plasmid transfection of erythroid cell lines and HSPCs

One million cells were transfected with 4 ug of the Cas9-GFP plasmid (pMJ920) and 0.8-1.6 µg of each sgRNA plasmid (MLM3636 or MA128) in a 100 µl volume using Nucleofector I (Lonza). We used AMAXA Cell Line Nucleofector Kit V (VCA-1003) for K562 and HUDEP-2 (T-16/U-16 and L-29 programs, respectively), and AMAXA Human CD34 Cell Nucleofector Kit (VPA-1003; U-08 program) for HD HSPCs. GFP^+ HUDEP-2 cells and GFP^+ HSPCs were FACS-sorted using SH800 Cell Sorter (Sony Biotechnology). As control, we used untreated cells, cell transfected only with Cas9-GFP plasmid or cells transfected only with nuclease-free TE buffer (10mM Tris and 1mM EDTA, pH 8).

CFC Assay

In the Colony Forming Cell (CFC) assay, SCD HSPCs were plated at a concentration of $2x10^3$ cells/ml in a methylcellulose-based medium (GFH4435, Stem Cell Technologies, Vancouver, BC, USA). BFU-E and CFU-GM colonies were counted 14 days after plating. BFU-E colonies were randomly picked and collected as bulk populations (containing at least 25 colonies) to evaluate the LV transduction and editing efficiencies.

Vector copy number analysis

HUDEP-2 cells and HSPC-derived mature erythroblasts were collected at day 9 and 13 of erythroid differentiation, respectively. BFU-E pools were collected 14 days after HSPC plating in the methylcellulose medium. Genomic DNA (gDNA) was extracted using PURE LINK Genomic DNA Mini kit (Life Technologies) following manufacturer's instructions. VCN per diploid genome was determined by digital droplet polymerase chain reaction (ddPCR), using the droplet reader QX200

droplet reader (Biorad), as previously described[9]. Fifty ng of gDNA was digested with 20 unit of DraI enzyme (New England BioLabs) in a total volume of 6 µL for 30 min at 37°C. We used 6 µL of the restriction mixture for the subsequent ddPCR analysis. We used primers and probes specific for: (i) the viral Ψ (PSI) packaging signal (HIV1-PSI FOR 5'-TCCCCCGCTTAATACTGACG-3', HIV1-PSI REV 5'-CAGGACTCGGCTTGCTGAAG-3', HIV1-PSI PROBE FAM 5'-CGCACGGCAAGAGGCGAGG-3'); (ii) the human albumin gene (*ALB*), as an internal reference standard (ALB FOR 5'-GCTGTCATCTCTTGTGGGCTGT-3', ALB REV 5'-ACTCATGGGAGCTGCTGGTTC-3', ALB PROBE VIC 5'-CCTGTCATGCCCACACAAATCTCTCC-3'). The VCN was determined with the QuantaSoft software by calculating the ratio between the target molecule concentration and the reference molecule concentration multiplied by the number of copies of reference species in the genome.

PCR-based assays for detection of genome editing events

Genomic DNA was extracted using PURE LINK Genomic DNA Mini kit (Life Technologies) following manufacturer's instructions. To evaluate editing efficiency at sgRNA on-target and off-target sites (predicted using COSMID; OT 1 to OT 13, **Supplementary Table 2**), we performed PCR followed by Sanger sequencing and TIDE (Tracking of InDels by Decomposition)[10,11] or Synthego Performance ICE Analysis[2]. Primer sequences used for PCR analysis are listed in **Supplementary Table 3**.

Name	Target sequence	Mismatches	Hg19 genomic location	Strand	COSMID score	Type	Gene
HBB	TCTGCCGTTACTGCCCTGT	-	chr11:5,226,973-5,226,994	-	N/A	exon 1	HBB
HBD	ACTGCTGTCAATGCCCTGT	4	chr11:5,234,385-5,234,407	-	N/A	exon 1	HBD
HBG	GGCTACTATCACAAGCCTGT	8	chr11:5,249,756-5,249,778	+	N/A	exon 1	HBG1/2
OT 1	TCTGCCATTCTGCCCTGT	2	Chr8:38,506,485-38,506,505	-	1.48	intergenic	
OT 2	TCTGCTGTTATGCCCTGT	2	Chr5:121558627-121558647	+	2.24	intergenic	
OT 3	TCTGCCCTTACTGTCCTGT	2	Chr19:1379110-1379131	+	2.17	intergenic	
OT 4	GTTGCCGTTACTGCCCTCT	3	Chr10:83,375,539-83,375,561	+	5.28	intergenic	
OT 5	TCTGCCGTTTACTGCCCTGT	1	Chr1:162859324-162859346	+	21.05	intergenic	
OT 6	TCTGCCGTTCTGCCCTGT	1	Chr8:10621755-10621775	-	21.21	intron 5	SOX7
OT 7	TCAGCAGATACTGCCCTGT	3	Chr1:160398097-160398118	-	0.75	exon 8	VANGL2
OT 8	CCTGCCTGTTACTGCCCTGT	2	Chr11:28827844-28827866	+	1.1	intergenic	
OT 9	TCTGCCTTTCTGCCCTGT	2	Chr7:101091535-101091555	+	1.48	intron 3	COL26A1
OT 10	TCTGCCCTTCCTGCCCTGC	3	Chr12:48176342-48176363	-	6.97	exon 3	SLC48A1
OT 11	TCAGCCATTACTGCCCTGT	2	Chr7:127238493-127238514	-	20.44	exon 4	FSCN3
OT 12	TCTGCCGTTACTTCCCTGC	2	Chr14:89076092-89076113	+	27.3	exon 15	ZC3H14
OT 13	TCTGCCGATAGTGCCCTGT	2	Chr17:17636353-17636374	-	1.15	intron 2	RAI1

Supplementary Table 2: List of the potential off-target loci for gR-C. Putative off-target sequences for gR-C in *HBD* and *HBG* genes and top-13 off-target loci predicted by COSMID[12]. Mismatches between the on-target *HBB* sequence and off-targets are underlined.

Name	Orientation	Primer sequence (5' to 3')
HBB	Fwd	CAGTGCAGCTCACTCAGGTGT
	Rev	ACTCCTAAGCCAGTGCCAGA
HBAS3	Fwd	CAGTGCAGCTCACTCAGCTG
	Rev	ACTCCTAAGCCAGTGCCAGA
HBD	Fwd	TGAGCCAGGCCATCACTAAAGG
	Rev	CAGGGTTTCTGAGTCAAGACACAC
HBG	Fwd	CCTCTGGGTCCATGGGTAGA
	Rev	GCAGTATCCTCTTGGGGGCC
OT 1	Fwd	CAAGCCGTAGATGGAATCTCTTGG
	Rev	CCCAGGGAGAAAGGGAGAAAG

OT 2	Fwd	CAGTTTGAGCTGCTGAGGCAC
	Rev	GAGAACTGCTTTTGCTGCATCACG
OT 3	Fwd	TGGCCACACAGTGAGACTCC
	Rev	AAGCGTGCAGGCTTCTGAGG
OT 4	Fwd	TGCAAGATAGGGACAGAAGAAGCC
	Rev	GCCAGGAACATGGTAGACATTACG
OT 5	Fwd	TCCCCTCCCTGGTTTCACCAT
	Rev	ATCTGGCTAAGACATCCTGGCTC
OT 6	Fwd	GTCACCGAATTGGGGGCAAG
	Rev	AGGAGGTCCTCAGAAGGCTTAAG
OT 7	Fwd	CCCTCCCATTTCAGCCCTTAAC
	Rev	CAACAGAATGCCCCCACAAAAGTC
OT 8	Fwd	TCTTCCTGGCCCAGAACTGTTCC
	Rev	CAGAATAGAGGTCGGGGATTGAG
OT 9	Fwd	CACCGAGGCAGGTCCTAGTT
	Rev	AGGAGTTCGAGGCTGCAGTG
OT 10	Fwd	AGCGTGTGTGTGAGTGAGGC
	Rev	GGGAAGGAGCCATCAACAGTG
OT 11	Fwd	TCTCTCCCTATGATATCCTGGCG
	Rev	TGGGGTTTCACGTGGTCAGG
OT 12	Fwd	TGAACAGTTTCAGACCACTTGGCC
	Rev	CTCCAAAACCAGGTGAGTGAGTG
OT 13	Fwd	GTCCTGCTGCCCAGCTTGTT
	Rev	CTCCTTATCTTTCCCCACGCAG
BCL11A	Fwd	TGGACAGCCCGACAGATGAA

	Rev	AAAAGCGATACAGGGCTGGC
13bpdel	Fwd	AAAAACGGCTGACAAAAGAAGTCCTGGTAT
	Rev	ATAACCTCAGACGTTCCAGAAGCGAGTGTG

Supplementary Table 3: List of primers for on-target and off-target analyses. Primers used to amplify the on-target loci of gR-A, gR-B, gR-C, gR-D, gR-BCL11A and gR-13bpdel, and the top-predicted off-target loci of gR-C. HBD primers were also used to evaluate the potential off-target activity of gR-D at the *HBD* gene. Fwd: forward and Rev: reverse.

GUIDE-seq and deep-sequencing analysis of off-target loci

GUIDE-seq was performed in HEK293 cells as previously described [13,14]. Off-targets identified by GUIDE-seq were PCR-amplified using the Phusion High-Fidelity Taq polymerase with GC Buffer (New England BioLabs). Primer sequences used to amplify off-targets identified by GUIDE-seq are listed in **Supplementary Table 4.** We performed PCR followed by deep sequencing analyses as previously described[15]. Briefly, Illumina compatible barcoded DNA amplicon libraries were prepared using the TruSeq DNA PCR-Free kit (Illumina). Libraries were pooled and sequenced using Illumina HiSeq2500 (paired-end sequencing 130 130 bases). A total of 0.59 to 1.12 million passing filter reads per sample were produced. Targeted deep-sequencing data were analyzed using CRISPRESSO [16]. The GUIDE-seq datasets are available in the BioProject repository under the accession number PRJNA734605.

Name	Orientation	Primer sequence (5' to 3')
chr 9	Fwd	CTCCCAAATTGAAAGCACAGCCAG
	Rev	TTTCCCGTTCTCCACCCAATAGC
chr 10	Fwd	TGGAGAAAGACAATGGCAGTGAGG
	Rev	CTAGCACTGCCCCACAATAGTAC

chr 6	Fwd	CCAGCATCACTACCAAGTCTCC
	Rev	AAAATCCCCCCACGGATGCC
chr 3	Fwd	CCCTAAGATTGTGGTTCCTTAGCC
	Rev	CAGGATTACTTGGGCAGAGACTAC
chr 17	Fwd	GGAATGACTGAATCGGAACAAGG
	Rev	CTGGCCTCACTGGATACTCT

Supplementary Table 4. Primers used to amplify putative off-targets of gR-C (chr 9, 10, 6 and 3) or gR-13bpdel (chr 17). Fwd: forward and Rev: reverse.

Quantitative RT-PCR (qRT-PCR)

Total RNA was extracted using RNeasy micro kit (QIAGEN) following manufacturer's instructions. Mature transcripts were reverse-transcribed using SuperScript First-Strand Synthesis System for RT-PCR (Invitrogen) with oligo(dT) primer. qRT-PCR was performed using an iTaq Universal SYBR green master mix (Bio-Rad) and Viia7 Real-Time PCR system (Thermo Fisher Scientific). Primer sequences are listed in **Supplementary Table 5**.

Gene	Orientation	Sequence (5' to 3')
HBA	Fwd	CGGTCAACTTCAAGCTCCTAA
	Rev	ACAGAAGCCAGGAACTTGTC
HBB	Fwd	AAGGGCACCTTTGCCACA
	Rev	GCCACCACTTTCTGATAGGCAG
HBAS3	Fwd	AAGGGCACCTTTGCCCAG
	Rev	GCCACCACTTTCTGATAGGCAG
HBG1/2	Fwd	CCTGTCCTCTGCCTCTGCC

	Rev	GGATTGCCAAAACGGTCAC
GAPDH	Fwd	GAAGGTGAAGGTCGGAGT
	Rev	GAAGATGGTGATGGGATTTC
BCL11A-XL	Fwd	ATGCGAGCTGTGCAACTATG
	Rev	GTAAACGTCCTTCCCCACCT

Supplementary Table 5. List of primers used for qRT-PCR.

Flow cytometry analysis

We labeled HUDEP-2 cells and HSPC-derived erythroblasts with antibodies against CD36 (CD36-V450, BD Horizon), CD71 (CD71-FITC, BD Pharmingen), CD235a (CD235a-APC, BD Pharmingen; CD235a-PECY7, BD Pharmingen), CD49d (CD49d-APC, BD Bioscience) and Band3 (Band3-PE, Bristol Institute for Transfusion Sciences) surface markers. We used the nuclear dye DRAQ5 (eBioscience, 0.1/100 dilution) to evaluate the proportion of enucleated RBCs.

Differentiated cells were fixed and permeabilized using BD Cytofix/Cytoperm solution (BD Pharmingen) for HUDEP-2 cells and glutaraldehyde and Triton 1X for HSPCs-derived erythroblasts. After permeabilization, cells were stained with antibodies recognizing HbF (HbF-APC, MHF05, Life Technologies and HbF-FITC, 552829, BD Pharmingen, 1/100 dilution).

We performed flow cytometry analyses using Fortessa X20 flow cytometer (BD Biosciences) and Gallios (Beckman Coulter).

Western blot

Differentiated HUDEP-2 cells (9 days of differentiation; 2-3x10^6 cells) were collected and resuspended for 30 min at 4°C in a lysis buffer containing: 10mM Tris, 1 mM EDTA, 0.5mM EGTA, 1% Triton X-100, 0.1% SDS, 0.1% Na-deoxicholate, 140mM NaCl (Sigma-Aldrich) and protease inhibitor cocktail (Roche-Diagnostics). Cell lysates were sonicated twice (50% amplitude, 10 sec per cycle, pulse 9 sec on/1 sec off) and underwent 3 cycles of freezing/thawing (3 min at -80°C/3 min at

37°C). Lysates were centrifuged at 12.000 x g for 10 min at 4°C, and supernatants were used as protein extracts for biochemical analysis. Protein concentration was measured using the Pierce™ BCA Protein Assay Kit (ThermoScientific). 25 µg of samples were loaded on a 15% (wt/vol) Sodium Dodecyl Sulphate (SDS)-PAGE gel and transferred onto PVDF membranes (Millipore) pre-activated in ethanol, using a Mini Blot Transfer Module (Thermo). After transfer, membranes were incubated for 1 hour in Tris-buffered saline (TBS)-Tween buffer (50 mM Tris-HCl pH8, 150 mM NaCl, 0.1% Tween 20 in water) completed with 5% skim milk. Immunoblots were carried out over-night at 4°C in a solution containing 3% (wt/vol) BSA in TBS with a mouse antibody recognizing β-globin (1:200; sc-21757, SantaCruz) or a goat antibody against α-globin (1:200; sc-31110, SantaCruz). Blots were washed and incubated with peroxidase-conjugated donkey anti-mouse (1:10,000) or donkey anti-goat (1:5,000) antibody for 60 min at RT. After washing, blots were incubated with enhanced chemiluminescent (ECL) substrate (Pierce) and exposed to film (Amersham) that was developed following manufacturer's instructions. Images were quantified by using Gel-Pro analyzer 4.0 (Media Cybernetics).

Keywords

Lentiviral vectors, genome editing, CRISPR/Cas9 nuclease, sickle cell disease.

References

1. Romano O, Petiti L, Felix T, et al. GATA Factor-Mediated Gene Regulation in Human Erythropoiesis. *iScience*. 2020;23(4):.

296 2. Hsiau T, Conant D, Rossi N, et al. Inference of CRISPR Edits from Sanger Trace Data.
297 *BioRxiv*. 2018;
298 3. Dang Y, Jia G, Choi J, et al. Optimizing sgRNA structure to improve CRISPR-Cas9 knockout
299 efficiency. *Genome Biology*. 2015;15;16:280.
300 4. Cottle RN, Lee CM, Archer D, Bao G. Controlled delivery of β-globin-targeting TALENs and
301 CRISPR/Cas9 into mammalian cells for genome editing using microinjection. *Sci Rep*. 2015;5:.
302 5. Liang P, Xu Y, Zhang X, et al. CRISPR/Cas9-mediated gene editing in human tripronuclear
303 zygotes. *Protein Cell*. 2015;6(5):363–372.
304 6. Huang X, Wang Y, Yan W, et al. Production of Gene-Corrected Adult Beta Globin Protein in
305 Human Erythrocytes Differentiated from Patient iPSCs After Genome Editing of the Sickle Point
306 Mutation: Corrected β Globin in Genome-Edited Human iPSCs. *Ste*. 2015;33(5):1470–1479.
307 7. Kurita R, Suda N, Sudo K, et al. Establishment of Immortalized Human Erythroid Progenitor
308 Cell Lines Able to Produce Enucleated Red Blood Cells. *PLoS One*. 2013;8(3):.
309 8. Antoniani C, Meneghini V, Lattanzi A, et al. Induction of fetal hemoglobin synthesis by
310 CRISPR/Cas9-mediated editing of the human β-globin locus. *Blood*. 2018;131(17):1960–1973.
311 9. Lin H-T, Okumura T, Yatsuda Y, et al. Application of Droplet Digital PCR for Estimating
312 Vector Copy Number States in Stem Cell Gene Therapy. *Hum Gene Ther Methods*. 2016;27(5):197–
313 208.
314 10. Brinkman EK, van Steensel B. Rapid Quantitative Evaluation of CRISPR Genome Editing by
315 TIDE and TIDER. *Methods Mol. Biol.* 2019;1961:29–44.
316 11. Brinkman EK, Chen T, Amendola M, van Steensel B. Easy quantitative assessment of genome
317 editing by sequence trace decomposition. *Nucleic Acids Res*. 2014;42(22):e168.
318 12. Cradick TJ, Qiu P, Lee CM, Fine EJ, Bao G. COSMID: A Web-based Tool for Identifying
319 and Validating CRISPR/Cas Off-target Sites. *Mol Ther Nucleic Acids*. 2014;3(12):e214.
320 13. Tsai SQ, Zheng Z, Nguyen NT, et al. GUIDE-seq enables genome-wide profiling of off-target
321 cleavage by CRISPR-Cas nucleases. *Nature Biotechnology*. 2015;33(2):187–197.

14. Weber L, Frati G, Felix T, et al. Editing a γ-globin repressor binding site restores fetal hemoglobin synthesis and corrects the sickle cell disease phenotype. *Sci. Adv.* 2020;6(7):eaay9392.

15. Lattanzi A, Meneghini V, Pavani G, et al. Optimization of CRISPR/Cas9 Delivery to Human Hematopoietic Stem and Progenitor Cells for Therapeutic Genomic Rearrangements. *Molecular Therapy*. 2018;

16. Pinello L, Canver MC, Hoban MD, et al. Analyzing CRISPR genome-editing experiments with CRISPResso. *Nature Biotechnology*. 2016;34(7):695–697.